of RNA by these antiviral proteins little affect host metabolism. However, no one has yet demonstrated such a compartment.

IFNs are not normally produced at biologically significant levels. Most types of mammalian cells are capable of producing IFN upon viral infection. Viral replication is sensed by cytoplasmic non-self RNA sensors; RIG-I, melanoma differentiation-associated gene 5 (MDA5), and laboratory of genetics and physiology 2 (LGP2), which are collectively termed RLRs, to initiate the cascade of events leading to the activation of transcription factors, IRF-3/-7 and nuclear factor-êB (NF-êB), then the activation of IFN genes [5–9]. Thus, the primary function of the IFN system is to sense non-self RNA and to eradicate the invading RNA, which includes RNA derived from the replication of DNA viruses [10,11]. Although genetic evidence shows that RLR is critical for detecting viral RNA in the cytoplasm, its specific distribution has been unknown.

In this report, we investigated the cellular localization of RIG-I in Influenza A Virus -infected cells. We discovered that viral infection or the transfection of viral RNA causes RIG-I to form granular aggregates containing stress granule markers, which we term antiviral stress granules (avSGs). Our analyses revealed that avSGs are critical for signaling to activate the IFN gene, suggesting that the avSG serves as a platform for the sensing of non-self RNA by RLRs. Furthermore, because the granule also recruits PKR, OAS and RNase L, it is strongly suggested to be the compartment where some antiviral proteins inhibit viral replication.

Results

Infection of NS1-deficient IAV Produces Granules Containing RIG-I

We generated an anti-RIG-I antibody, which specifically detects RIG-I by immunostaining and immunoblotting (Figure S1) (Materials and Methods) [12]. To observe the cellular distribution of RIG-I, cells were infected with two types of IAV, the wild type (WT) and ÄNS1 which lacks the gene for non-structural protein 1 (NS1), a potent inhibitor of IFN production [13]. WT IAV replication was detectable at 3 h after infection as a nuclear accumulation of viral nucleocapsid protein (NP) (Figure 1A). Later in the infection (9–12 h), NP, presumably as a complex with viral genomic RNA [14], translocated to the cytoplasm. RIG-I was dispersed in uninfected cells and WT IAV infection did not cause any change in its distribution. On the other hand, in cells infected with IAVÄNS1, NP accumulated in the nucleus at 6 h post-infection, however only a fraction of NP translocated to the cytoplasm at 9–12 h (Figure 1B). Unlike WT IAV, the NP of IAVÄNS1 exhibited a speckle-like distribution in the cytoplasm. Notably, formation of this RIG-I-containing speckle strongly correlates with activation of RIG-I-mediated signal activation as judged by nuclear localization (Figure 1C) and dimerization of IRF-3 and concomitant enhanced production of ISGs, such as RLRs and STAT1 (Data not shown). Indeed, the ratio of cells with IAV- and IAVÄNS1-induced nuclear IRF-3 was 2.7% and 33.7%, respectively, and cells containing RIG-I speckles together with nuclear IRF-3 were 0.0% (IAV) and 72.2% (IAVÄNS1).

IAVÄNS1-induced Granules Contain Both Stress Granule Marker and Anti-viral Proteins

We characterized the nature of these speckles by using various antibodies and found that interestingly, RIG-I exhibited co-localization with NP (83.5%) and a stress granule (SG) marker, T-cell restricted intracellular antigen-related protein (TIAR) (97.1%) at 9 h (Figure 1B). Other SG markers are similarly recruited to the granules produced by IAVÄNS1: Ras-GAP SH3 domain-binding protein (G3BP) (97.6% colocalized with RIG-I), eIF3 (99.8% colocalized with G3BP) (Figure 1D and 1E), and human antigen R (HuR) (98.8% colocalized with RIG-I) (data not shown). Furthermore, physical interaction between RIG-I and SG markers was demonstrated by pull-down assays (Figure 1F). These results strongly suggest that although IAV infection potentially induces signaling to activate the IFN gene and the formation of granular aggregates containing SG markers, NS1 strongly blocks both. Ectopic expression of full-length NS1 and the N-terminal RNA-binding domain of NS1 dramatically inhibited both granule-formation and RIG-I signaling in response to IAVÄNS1 infection, indicating that the N-terminal domain of NS1 is responsible for these activities (Figure S2A and S2B).

SGs are an intracellular ribonucleoprotein (RNP) complex generated by cellular stress, including oxidative, heat shock, and endoplasmic reticulum stress, and contain translation-stalled mRNAs and various RNA-binding proteins [15]. Because many of the SG markers are RNA-binding proteins, we examined the localization of other RLRs, MDA5, and LGP2, as well as PKR (see below), RNase L, and OAS by using specific antibodies. Interestingly, these proteins were also recruited to SG and virus-induced granules in response to arsenite and IAVÄNS1, respectively (Figure 2A, 2B, 2C, 2D).

IAVÄNS1 Infection Induces Antiviral SGs Containing Viral RNA

These results prompted us to examine correlation between the formation of SGs and activation of the IFN gene. Treatment of cells with arsenite ($NaAsO_2$), which induced oxidative stress, produced granules similar to those generated by IAVÄNS1 (Figure 3A). Similarly, artificial overexpression of PKR resulted in the formation of SGs (58.9%) (Figure 3A). Although IAVÄNS1 infection activated the IFN-â gene, neither arsenite nor PKR activated the gene (Figure 3B). These results suggest that SGs and virus-induced granules are functionally distinct, possibly due to the presence of viral RNA in virus-induced granules. Indeed, fluorescence *in situ* hybridization (FISH) clearly demonstrated that viral RNA colocalized with the granules of NP (Figure 3C) and RIG-I (Figure 3D) in IAVÄNS1-infected cells whereas IAV-infected cells showed colocalization of viral RNA with NP (Figure S3A) but not with RIG-I (Figure S3B). Once viral RNA is engaged by RIG-I-containing complex, IFN-â promoter stimulator-1 (IPS-1, also known as MAVS, VISA or Cardif) expressed on the outer membrane of mitochondria is recruited to facilitate RIG-I-IPS1 signaling in a Mitofusin 1-dependent manner [12,16]. Although most of IPS-1 localizes on mitochondrial network in uninfected and IAV-infected cells, IAVÄNS1 infection induces speckle-like distribution. The re-localized IPS-1 exhibits apparent contacts with TIAR- (Figure 3E, bottom-right panel), and RIG-I- (Figure S4) containing SGs. This is consistent with a model that SG physically contacts with mitochondrion mediated by interaction between RIG-I and IPS-1 through caspase recruitment domain (CARD)-CARD homotypic interaction [17–20]. Although association of FLAG-tagged IPS-1 with peroxisome membrane protein (PMP70)-positive peroxisomes after viral infection was reported [21], we did not observe their apparent association (Figure 3E).

SG production is not a result of RIG-I signaling or IFN signaling because overexpression of IPS-1 activated the nuclear translocation of IRF-3 without generating SGs (Figure S5A), and SGs formed in IFN receptor-deficient HEC-1B cells (Figure S5B). Furthermore, other viruses including Sindbis (SINV), encephalomyocarditis (EMCV), and Adeno (Ad) dl203 viruses also generated granules containing RIG-I and G3BP (Figure S5C), suggesting this SG-like granule to be a general response to viral infections. To

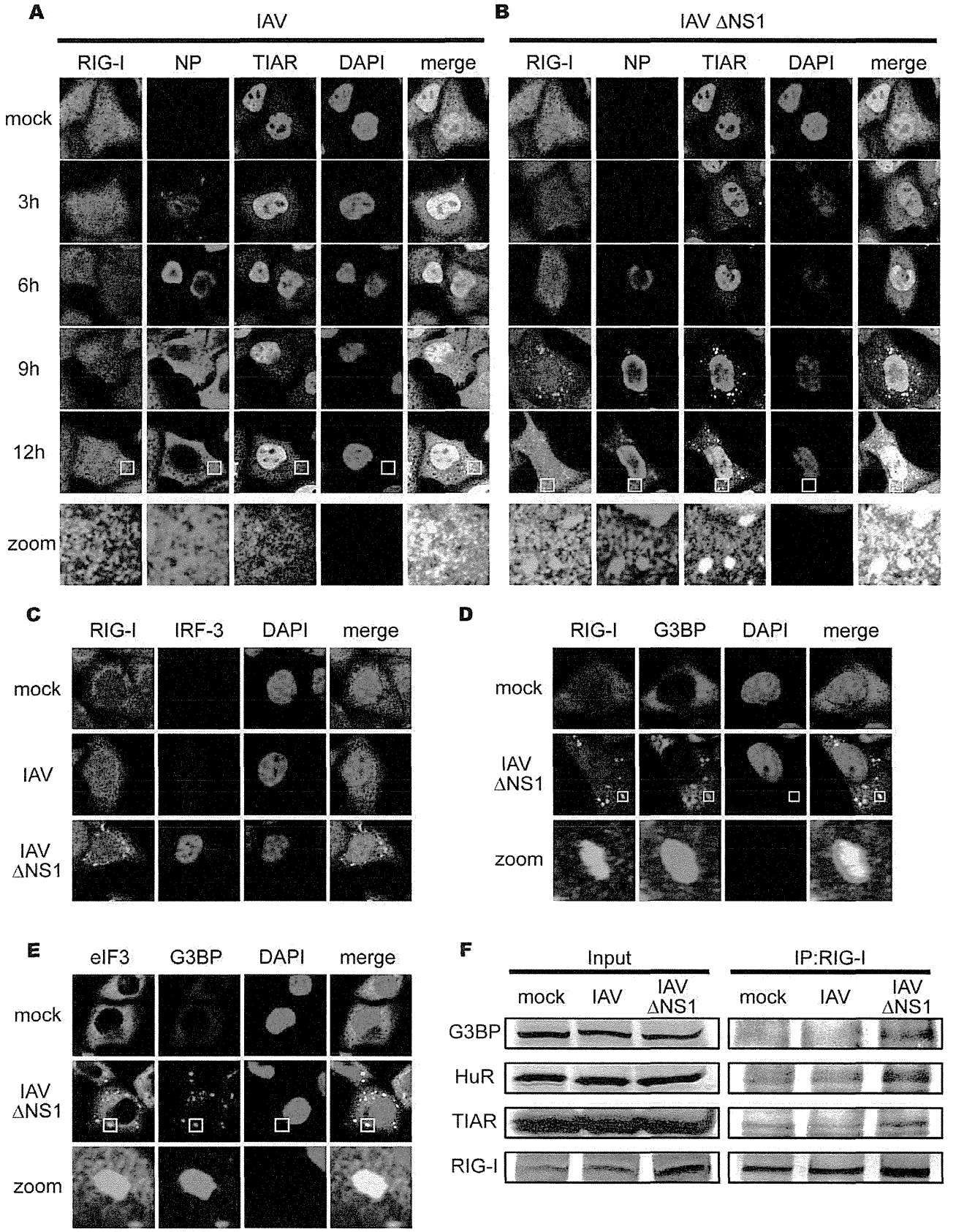

Figure 1. IAV infection causes a speckle-like distribution of RIG-I and stress granule markers. (**A–C**) HeLa cells were mock-treated or infected with IAV (**A**) or IAVÄNS1 (**B**) for the indicated period, fixed, stained, and analyzed with confocal microscopy. The cells were stained with anti-RIG-I (RIG-I), anti-IAV nucleocapsid protein (NP), and anti-TIAR (TIAR) antibodies. Nuclei were stained with DAPI. At 9 h and 12 h after infection, the

percentage of speckle-like distribution of RIG-I was 0.5% and 0.0% in IAV-infected cells, and 62.4% and 83.6% in IAVÄNS1-infected cells, respectively. The zoomed images correspond to the boxed region in each panel. The cells at 9 h post infection were stained with anti-RIG-I and anti-IRF-3 antibodies (**C**). (**D and E**) HeLa cells were infected with IAVÄNS1 for 9 h, and stained with anti-G3BP (G3BP), together with anti-RIG-I (RIG-I) (**D**) or anti-eIF3 (eIF3) (**E**). The zoomed images correspond to the boxed regions. (**F**) HeLa cells were mock-treated or infected with IAV or IAVÄNS1 for 12 h. Cell extracts were prepared and immunoprecipitated with anti-RIG-I antibody. The precipitates were analyzed by immunoblotting (IP:RIG-I) using antibody against G3BP, HuR, TIAR and RIG-I. Input: 1/50 of the extracts used for immunoprecipitation were analyzed similarly by immunoblotting.
doi:10.1371/journal.pone.0043031.g001

distinguish virus-induced granules from conventional SGs, we termed the virus-induced speckles as antiviral SGs (avSGs).

Impairment of Formation of avSGs Inhibits IAVÄNS1-induced IFN Activation

In order to address whether the formation of avSGs is required for IFN expression, we knocked down G3BP, a critical component for formation of the canonical SGs. G3BP siRNA clearly down-regulated G3BP expression (Figure 4A). Consistent with a previous study [22], the knockdown of G3BP strongly inhibited avSG formation in IAVÄNS1-infected cells (Figure 4B), and the number of cells which showed a speckle-like distribution of RIG-I and TIAR was diminished (Figure 4C and 4D). Moreover, IFN-â gene expression was strongly inhibited in G3BP knockdown cells compared to control siRNA-treated cells (Figure 4E). These results suggest that avSG formation is required for efficient activation of type I IFN. Furthermore, knockdown of eIF3 or RHAU, both of which are components of SG, also blocked both avSG formation and IFN gene activation (data not shown).

IAVÄNS1 Infection Induces PKR's Activation and Accumulation in avSGs

It has been proposed that a family of protein kinases including PKR, general control non-derepressible 2 (GCN2), PKR-like endoplasmic reticulum kinase (PERK), and heme-regulated eIF2á kinase (HRI) phosphorylate eIF2á, resulting in formation of SGs. Arsenite treatment causes oxidative stress leading to the activation of HRI, and SGs are produced. PKR is activated by dsRNA or 5¢ppp-containing RNA [23], therefore we speculate that the IAV RNA activates PKR resulting in the formation of avSGs via the phosphorylation of eIF2á. To address the involvement of PKR, we examined the localization of PKR in arsenite-treated and IAVÄNS1-infected cells and found that PKR accumulated in SGs and avSGs (Figure 5A). Interestingly, phosphorylated eIF2á was also detected in avSGs specifically generated by IAVÄNS1 but not in IAV-infected cells (Figure 5B). Immunoblotting confirmed that IAVÄNS1 specifically induced the phosphorylation of PKR and eIF2á whereas arsenite treatment induced the phosphorylation of eIF2á without PKR activation, indicating that IAVÄNS1 and arsenite induce SGs via distinct pathways (Figure 5C).

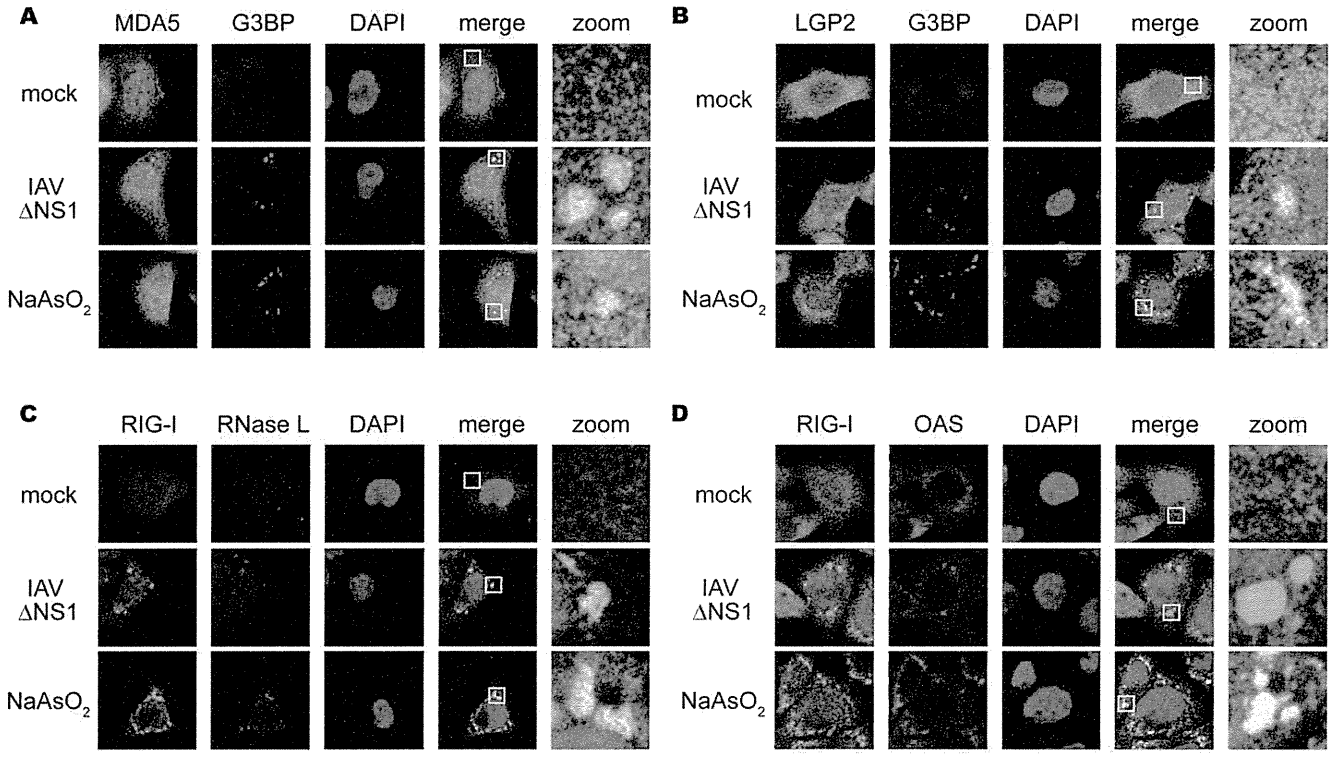

Figure 2. Antiviral proteins are colocalized with SGs. (**A–D**) HeLa cells were mock-treated (mock), infected with IAVÄNS1 for 9 h, or treated with $NaAsO_2$ for 1 h. Cells were fixed and stained for G3BP and MDA5 (94.2% colocalization) (**A**), G3BP and LGP2 (97.6% colocalization) (**B**), RIG-I and RNase L (84.5% colocalization) (**C**), RIG-I and OAS (87.4% colocalization) (**D**) in IAVÄNS1-infected cells. The zoomed images correspond to the boxed regions.
doi:10.1371/journal.pone.0043031.g002

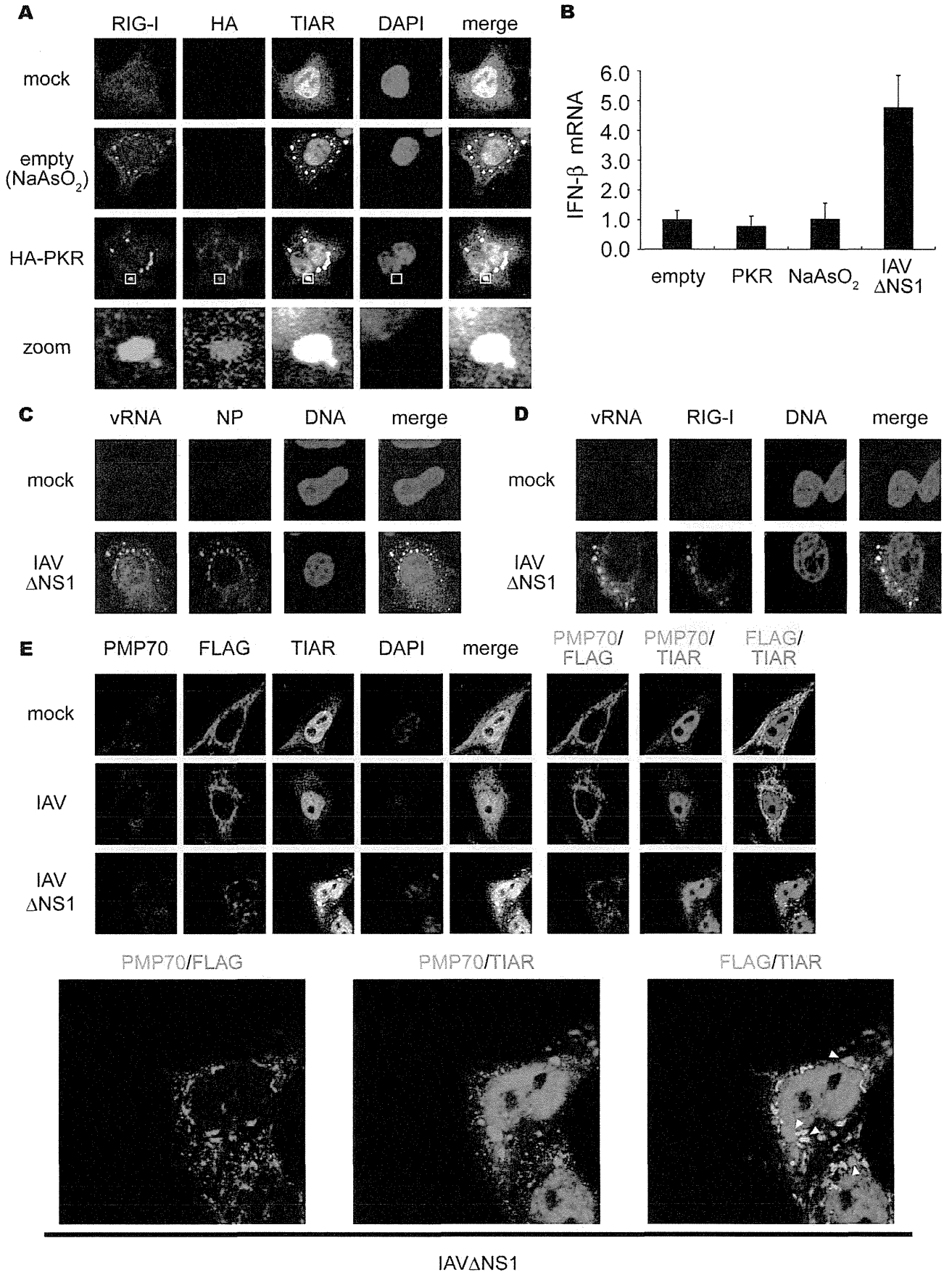
A
RIG-I
HA
TIAR
DAPI
merge
mock
empty
(NaAsO2)
HA-PKR
zoom
B
IFN-β mRNA
6.0
5.0
4.0
3.0
2.0
1.0
0.0
empty
PKR
NaAsO2
IAV
ΔNS1
C
vRNA
NP
DNA
merge
mock
IAV
ΔNS1
D
vRNA
RIG-I
DNA
merge
mock
IAV
ΔNS1
E
PMP70
FLAG
TIAR
DAPI
merge
PMP70/
FLAG
PMP70/
TIAR
FLAG/
TIAR
mock
IAV
IAV
ΔNS1
PMP70/FLAG
PMP70/TIAR
FLAG/TIAR
IAVΔNS1

Figure 3. Viral RNA is required for formation of functional SG to activate RIG-I/IPS-1 signaling pathway. (**A**) 293T cells were transfected with empty vector (empty) or the HA-PKR expression vector (HA-PKR) for 24 h, or treated with $NaAsO_2$ for 1 h and stained with anti-RIG-I, anti-HA (PKR) and anti-TIAR antibodies and DAPI. The zoomed images correspond to the boxed regions. (**B**) 293T cells were transfected with empty vector (empty), or the HA-PKR expression vector for 48 h, or treated with $NaAsO_2$ for 1 h, or infected with IAVÄNS1 for 12 h. Relative mRNA levels of endogenous IFN-â gene were determined by quantitative PCR (qPCR). Data are represented as the mean standard ± error of the mean (SEM). (**C and D**) HeLa cells were mock-treated or infected with IAVÄNS1 for 12 h. Viral RNA (vRNA) was detected by the FISH method using an RNA probe complementary to the segment 1 of the IAV, and NP (**C**) and RIG-I (**D**) were detected using anti-NP and anti-RIG-I antibodies (97.1%, and 98.2% colocalization of vRNA with NP and RIG-I, respectively). TO-PRO-3 was used for staining of nuclear DNA (DNA). (**E**) HeLa cell lines stably expressing FLAG-tagged IPS-1 were mock-treated or infected with IAV or IAVÄNS1 for 10 h. The cells were stained with anti-PMP70, anti-FLAG, and anti-TIAR antibodies. The white arrowheads indicated the contacts between FLAG-IPS-1 and TIAR. 67.8% of IAVÄNS1 infected cells exhibited contacts, whereas IAV infected cells hardly exhibited the contact (2.7%). The zoomed images of PMP70 (Green) and FLAG (Red), PMP70 (Green) and TIAR (Red), and FLAG (Green) and TIAR (Red) in IAVÄNS1-infected cells were shown in the bottom panel.
doi:10.1371/journal.pone.0043031.g003

Critical Role of PKR in avSG Formation and IFN Production in IAV-infected Cells

The results described above indicate the formation of viral RNA-containing avSGs to be essential to RLR-mediated antiviral signaling. To evaluate the requirement of PKR during IAVÄNS1 infection, we analyzed the formation of avSGs in mouse embryonic fibroblasts (MEFs) derived from WT and PKR knock-out (KO) mice (Figure 6). PKR WT and KO MEFs were infected with either IAV or IAVÄNS1, and stained with the anti-RIG-I, anti-NP, and anti-TIAR antibodies and calculated the frequency of avSGs. In the case of WT IAV, avSGs did not form in WT and KO MEFs as determined in Figure 1. IAVÄNS1 produced avSGs in WT but not in PKR KO MEFs (Figure 6A, 6B, 6C). Moreover, deletion of PKR resulted in a blockade of IFN-â gene expression (Figure 6D), production of IFN-â protein (Figure 6E), and IRF-3 dimerization (Figure 6F). Furthermore, we confirmed these results using siRNA targeting PKR expression in HeLa cells. The siRNA efficiently knocked down endogenous

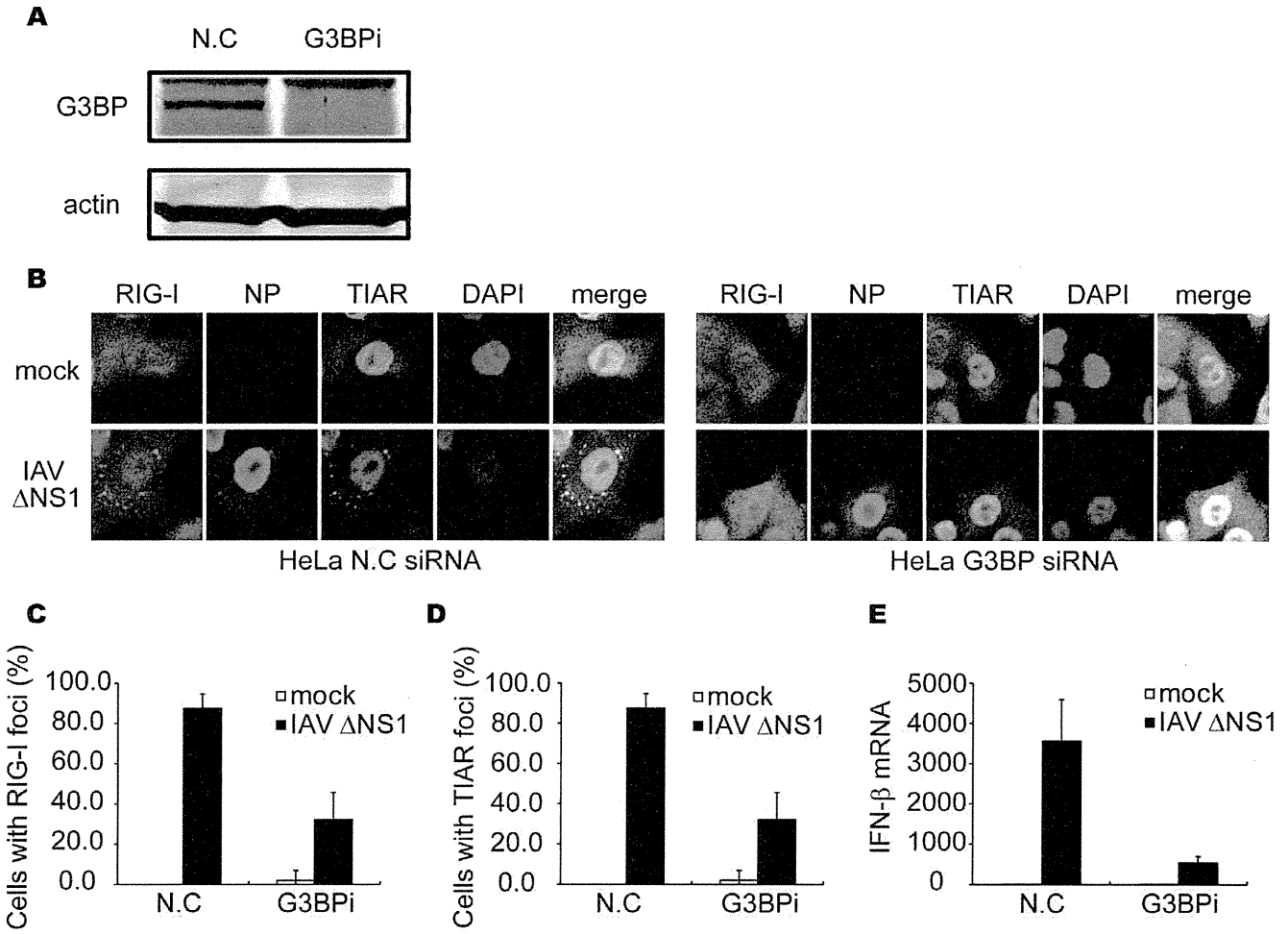

Figure 4. Knockdown of G3BP impairs formation of avSG and IFN-â gene activation. (**A–E**) HeLa cells were transfected with control siRNA (N.C) or siRNA targeting human G3BP (G3BPi). At 48 h after transfection, cells were harvested and G3BP and actin were detected by immunoblotting (**A**). Cells were mock-treated (mock) or infected with IAVÄNS1 for 12 h and fixed and stained with anti-RIG-I, anti-NP and anti-TIAR antibodies and DAPI (**B**). The percentage of cells containing foci of RIG-I (**C**) or TIAR (**D**) was determined. Relative mRNA level of IFN-â was determined by qPCR (**E**). Data are represented as the mean standard ± error of the mean (SEM).
doi:10.1371/journal.pone.0043031.g004

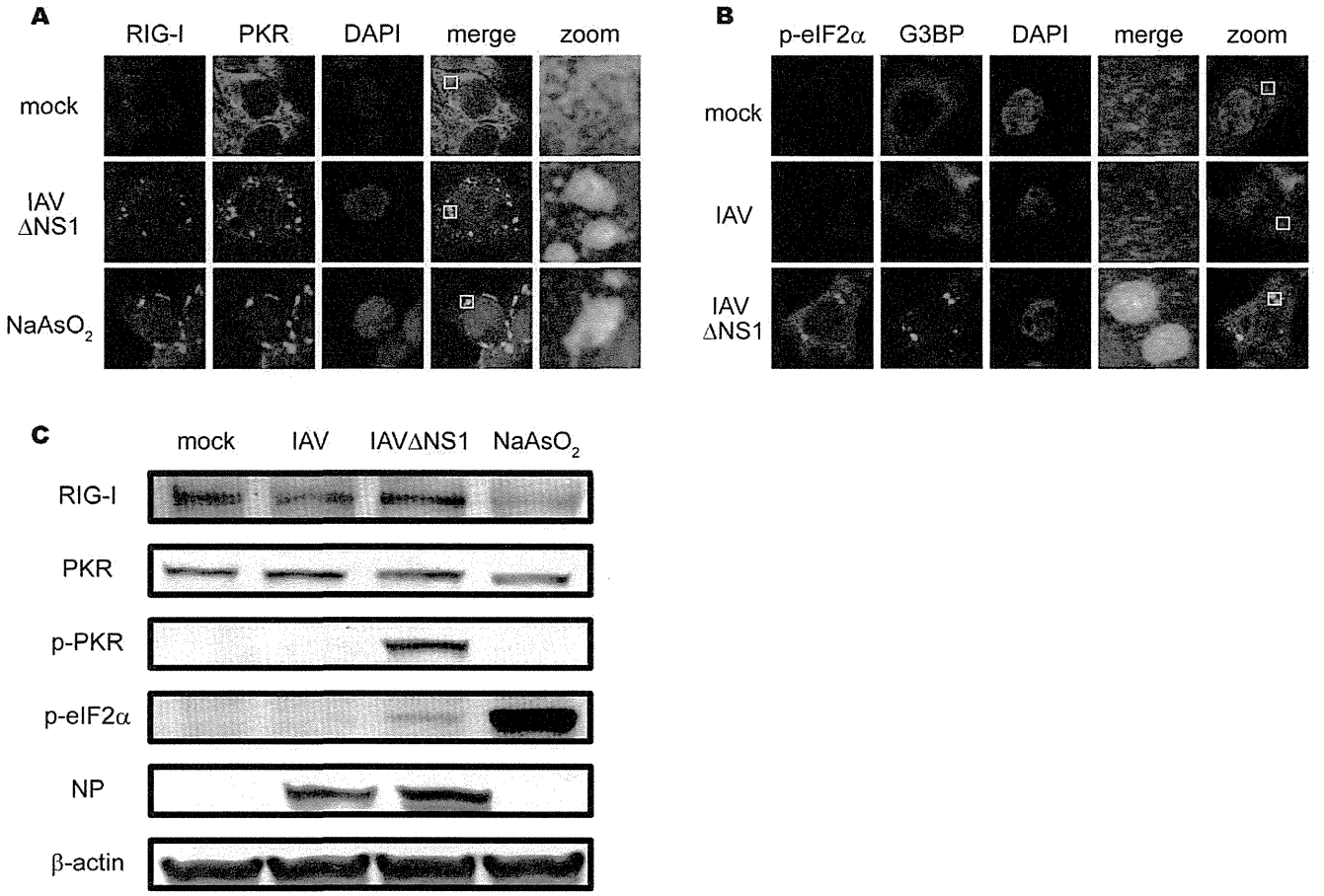

Figure 5. Localization and activation of PKR in IAVÄNS1-induced avSGs. (**A**) HeLa cells were mock-treated or infected with IAVÄNS1 for 9 h or treated with $NaAsO_2$ for 1 h. Cells were fixed and stained with anti-RIG-I and anti-PKR antibodies (% of colocalization: 95.1% and 97.0% in IAVÄNS1-infected and $NaAsO_2$-treated cells, respectively). The zoomed images correspond to the boxed regions. (**B**) HeLa cells were mock-treated or infected with IAV or IAVÄNS1 for 9 h and stained with anti-phospho-eIF2á (Ser 51) (p-eIF2á) and G3BP (% colocalization: 0.0% and 46.5% in IAV and IAVÄNS1-infected cells, respectively). The zoomed images correspond to the boxed regions. (**C**) HeLa cells were infected with IAV or IAVÄNS1 for 12 h or treated with $NaAsO_2$ for 1 h. Cell extracts were prepared and subjected to SDS-PAGE, and immunoblotted using antibodies against RIG-I, PKR, phosphorylated PKR (Thr 446) (p-PKR), phosphorylated eIF2á (Ser 51) (p-eIF2á), IAV NP, and â-actin.
doi:10.1371/journal.pone.0043031.g005

PKR expression, resulting in a strong inhibition of the IAVÄNS1-induced IFN-â gene expression, concomitant impairment of the number of avSG (Figure S6). Taken together, the results indicate that PKR is essential for avSGs and IFN gene activation in IAVÄNS1-infected cells. Importantly, blocking avSG formation by knockdown of PKR or G3BP enhanced the replication of IAVÄNS1 (Figure 7). These results strongly indicate a novel role for avSGs in the antiviral innate immune responses.

It is worth to note that in the absence of PKR, cytoplasmic transport of NP is accelerated (Figure 6A). This effect is also observed in HeLa cells in which PKR is knocked down (Figure S6C). Although the mechanism is unknown, these results suggest that PKR negatively regulate cytoplasmic transport of IAV nucleocapsid.

Viral RNA Generates avSGs in a PKR-dependent Manner

Previous reports showed that genomic RNA of IAV is responsible for triggering antiviral signaling via RIG-I [6,9,24,25]. Because the IAV genome is not infectious, we extracted it from the IAV-infected cells and transfected it into WT or PKR KO MEFs, and investigated whether the IAV genomic RNA solely induces the formation of avSGs and subsequent activation of the IFN gene. As shown in Figure 8A, the IAV genomic RNA is sufficient to produce avSGs, indicating that neither viral protein nor viral RNA replication is required. Furthermore, PKR is required for the formation of viral RNA-induced avSGs (Figure 8A and 8B). Because PKR is also required for poly I:C-induced IFN gene activation [26], we tested short and long poly I:C, which selectively activate RIG-I and MDA5, respectively [27]. Short and long poly I:C induced the formation of avSGs in a PKR-dependent manner (Figure 8A and 8B). We confirmed that IFN-â production by these RNA is PKR-dependent (Figure 8C). Viral but not host RNA is capable of triggering the response, as demonstrated by the finding that total RNA extracted from infected cells but not uninfected cells induced the formation of avSGs and activation of the IFN-â gene (Figure S7A and S7B). These findings demonstrate that PKR is necessary for formation of avSGs which recruits viral RNA and RLRs to trigger IFN gene activation during the IAV-infection. Of note, as shown in Figure 3B, overexpression of PKR can activate SG formation but not IFN expression in the absence of viral RNA, suggesting that function of PKR is prerequisite but insufficient for efficient induction of RLR-mediated antiviral signaling.

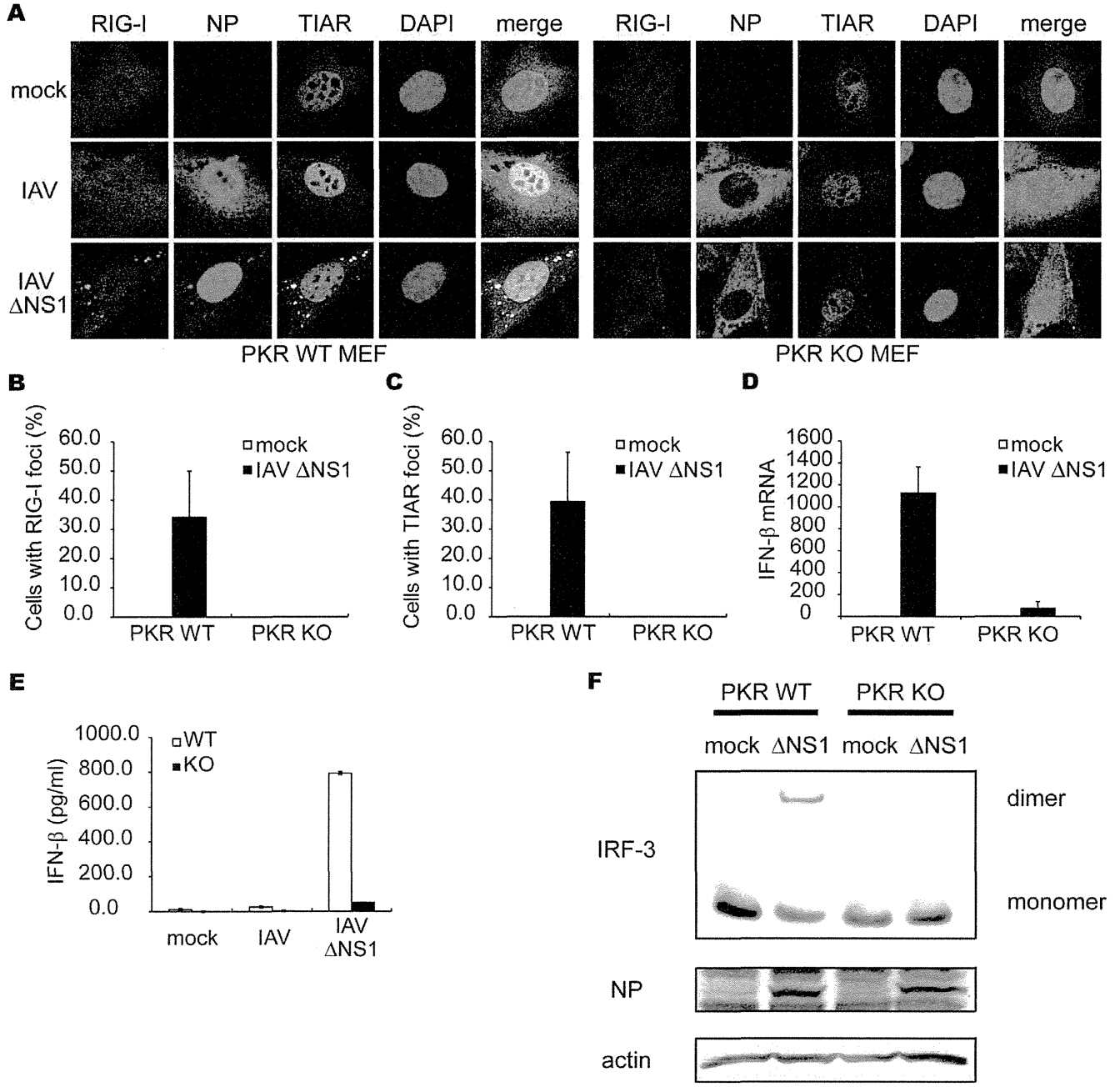

Figure 6. Critical role of PKR in formation of avSG and IFN-â gene activation. (**A–C**) MEFs derived from WT and PKR KO mice were mock-treated or infected with IAVÄNS1 for 12 h. The cells were stained with anti-RIG-I, anti-IAV NP and anti-TIAR antibodies and DAPI (**A**). The percentage of cells containing foci of RIG-I (**B**) or TIAR (**C**) was determined. (**D–F**) PKR WT and PKR KO MEFs were mock-treated or infected with IAVÄNS1. The IFN-â mRNA level at 9 h post-infection was determined by qPCR (**D**). The IFN-â protein levels in culture medium at 15 h post-infection were quantified by ELISA (**E**). Cell extracts were subjected to Native-PAGE and IRF-3 dimer was detected by immunoblotting using anti-IRF-3 antibody. IAV NP and actin were detected by SDS-PAGE followed by blotting using anti-NP and anti-actin antibodies (**F**). Data shown in B-E are represented as the mean standard ± error of the mean (SEM).
doi:10.1371/journal.pone.0043031.g006

Discussion

Recent studies have identified the domain structure of RLRs and the various adaptor proteins regulating RLR-mediated antiviral signaling cascades [28], but how RLRs encounter viral RNA in infected cells remain unclear. In this study, we found that all RLRs are recruited into cytoplasmic granules, termed avSGs, upon viral infections. avSGs contain many SG markers, G3BP, TIAR, and eIF3, but unlike canonical SGs, also contained viral RNA and viral NP. We demonstrated that avSGs are critical to virus-induced IFN gene activation. Since RLRs must efficiently find their ligands to act as vital sensors for viral RNA, avSGs may facilitate a proper encounter between viral RNA and RLRs. In addition, OAS and RNase L are recruited to avSGs, supporting the model that RNase L amplifies IFN-inducing signaling by unearthing cryptic ligands for RIG-I and MDA5 [29]. Further-

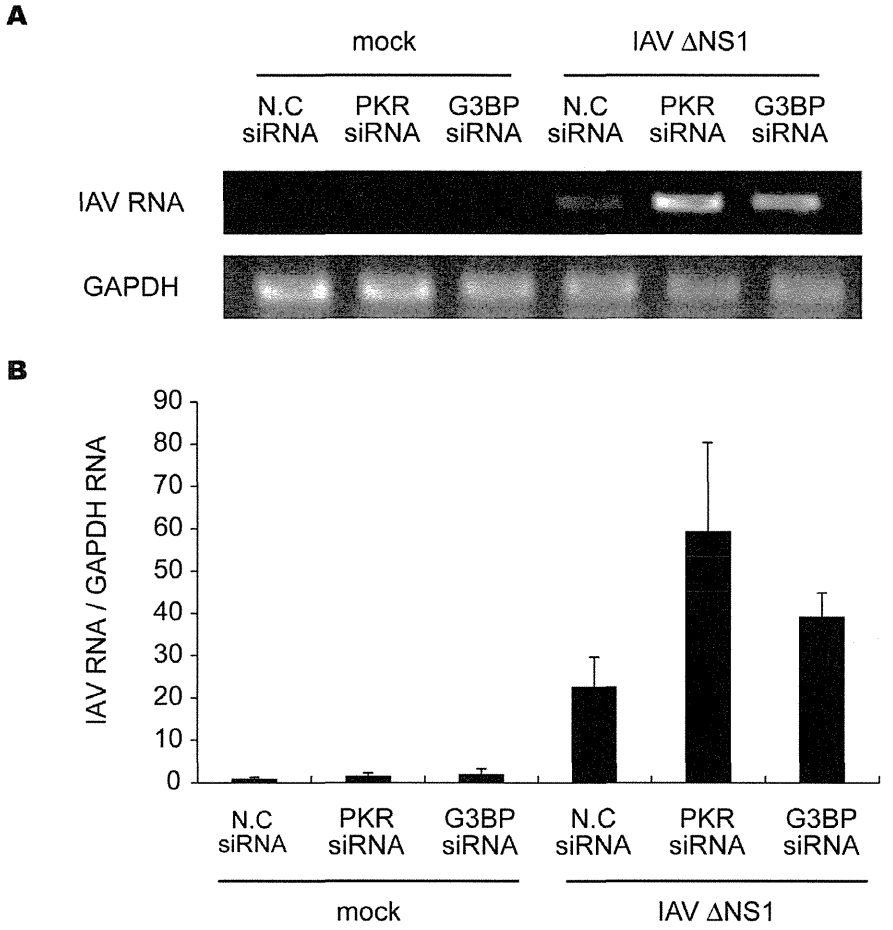

Figure 7. Inhibition of avSG formation enhanced IAV viral replication. HeLa cells were transfected with control siRNA (N.C) or siRNA targeting human PKR mRNA or G3BP. At 48 h after transfection, cells were mock-treated or infected with IAVÄNS1 for 24 h. The expression levels of IAV RNA segment 3 and GAPDH mRNA were determined by RT-PCR (**top**). The IAV RNA expression patterns were quantified with LAS-1000 UV mini (Fujifilm, Japan) and normalized with GAPDH (**bottom**). Data are represented as the mean standard ± error of the mean (SEM).
doi:10.1371/journal.pone.0043031.g007

more, the specific recruitment of antiviral proteins in avSGs suggests a critical role in the blocking of viral replication without an effect on host normal translation. We also observed that other viruses including SINV, EMCV Adenovirus, Hepatitis C virus and Newcastle disease virus induced avSG (Figure S5C and data not shown), suggesting that avSGs may function as a general platform for detection of many viruses to initiate antiviral signaling. Because PKR alone cannot trigger IFN gene activation (Figure 3B), PKR contributes at upstream of IAV-induced RIG-I activation. It was reported that SINV activates GCN2 to phosphorylate eIF2á [30], suggesting that the several viruses may activate different eIF2á kinases to form avSG.

Our model for the function of avSGs is summarized in Figure 9. We do not strictly rule out a possibility that PKR may directly phosphorylate target molecules to participate IFN gene activation, however because activation of PKR alone is not sufficient to trigger IFN production, this effect may be incremental.

Recognition of viral RNA by RIG-I and MDA5 induces ATP-dependent conformational change of the molecules and allows them to interact with mitochondrial IPS-1 via CARD-CARD interaction. Several reports indicated that activated RIG-I forms dimer or oligomer, which is required for efficient signal activation [31,32]. Furthermore, it was demonstrated that IPS-1 is redistributed on mitochondria in response to viral infection and IPS-1 forms prion-like aggregates [12,16]. These observations suggest a possibility that local enrichment of both RLRs and IPS-1 is required for signaling. Although our attempt to detect biochemical interaction between RLR-containing avSG and IPS-1 aggregates *in vitro* has been unsuccessful so far because of insoluble property of them, our immunohistochemical analysis strongly indicates that IPS-1-enriched mitochondria are physically attached with avSG in response to IAVÄNS1 infection (Figure 3E and S4), suggesting critical role of avSG as a platform for RLR-IPS-1 interaction.

The phosphorylation of eIF2á at Ser51 is known to trigger the formation of canonical SGs, however the precise mechanism by which the phosphorylated eIF2á recruits other SG components is not well understood because of difficulty of biochemical analysis [33]. We demonstrated that PKR was activated, recruited to avSGs, and essential for avSGs to form after IAVÄNS1 infection. Viral RNA is primarily responsible for triggering the PKR activation because transfection of IAV genomic RNA or poly I:C induced avSG formation and IFN gene activation in a PKR-dependent manner. Consistent with our data, some studies revealed that PKR deficiency impair production of IFN in response to polyI:C and viral infections [34–38]. Schulz et al. reported that PKR is not required for production of IFN-á/â proteins in response to IAV in bone marrow-derived dendritic cells (BM-DCs) [39]. This is apparently inconsistent with our data

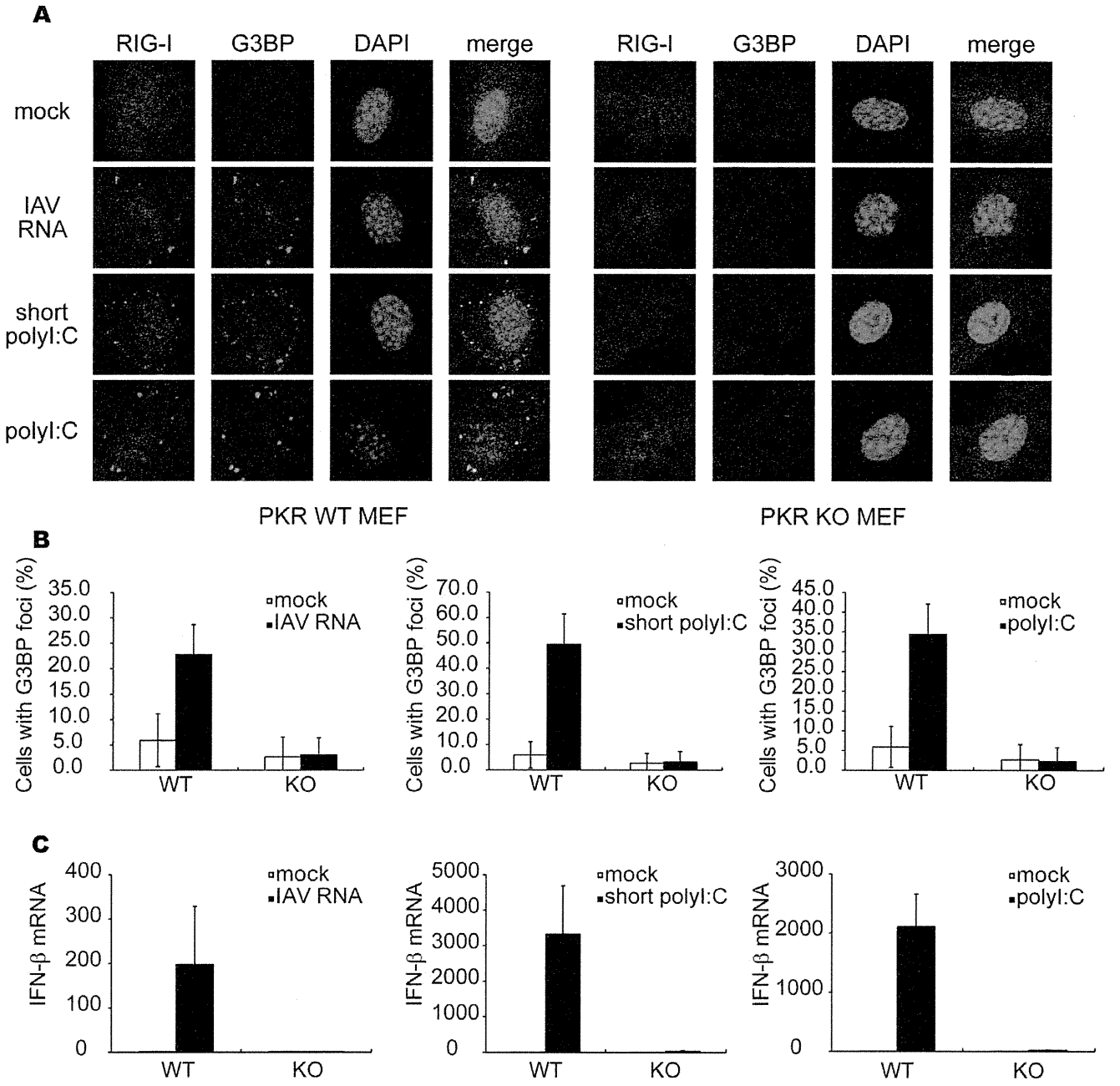

Figure 8. Viral RNA and polyI:C induce formation of avSGs and IFN-â gene expression in a PKR-dependent manner. (**A–C**) MEFs derived from WT and PKR KO mice were mock-treated or transfected with IAV genomic RNA, short poly I:C or long poly I:C for 9 h and stained with anti-RIG-I, anti-G3BP antibodies and DAPI (**A**). The percentage of cells containing foci of G3BP was shown in (**B**). Relative IFN-â mRNA levels were determined by qPCR (**C**). Data shown in B and C are represented as the mean standard ± error of the mean (SEM).
doi:10.1371/journal.pone.0043031.g008

obtained with MEFs. Although we were unable to directly compare between MEF and BM-DC, our explanation for this discrepancy is cell type difference, because IFN protein expression as determined by ELISA (Figure 6E) is consistent with mRNA level (Figure 6D) and PKR knockdown with HeLa cells dramatically diminished IFN production (Figure S6B). BM-DC may utilize eIF2á kinase other than PKR to form avSG.

The NS1 of IAV is a multifunctional protein that inhibits various host factors, including PKR [40,41], RIG-I [42,43], and tripartite motif-containing protein 25 (TRIM25), known to regulate RIG-I activation [44], and potentially sequesters viral dsRNA through its dsRNA-binding domain. Here, we demonstrated that NS1 of IAV markedly inhibited avSGs and the IFN gene's activation. Consistently, a recent report demonstrated that formation of IAV-induced SG was inhibited by wild type NS1, but not by mutant NS1, in which Arg38 and Arg41 are substituted to Ala [41]. Several classes of viruses are known to inhibit the formation of SGs during infection. The West Nile and Sendai viruses encode RNA that interacts with TIAR and inhibits SG assembly [45,46]. The poliovirus 3C protease cleaves G3BP at Gln 326 during the infection process [22]. Moreover, Simpon-Holley et al. recently demonstrated that the E3L protein of Vaccinia virus

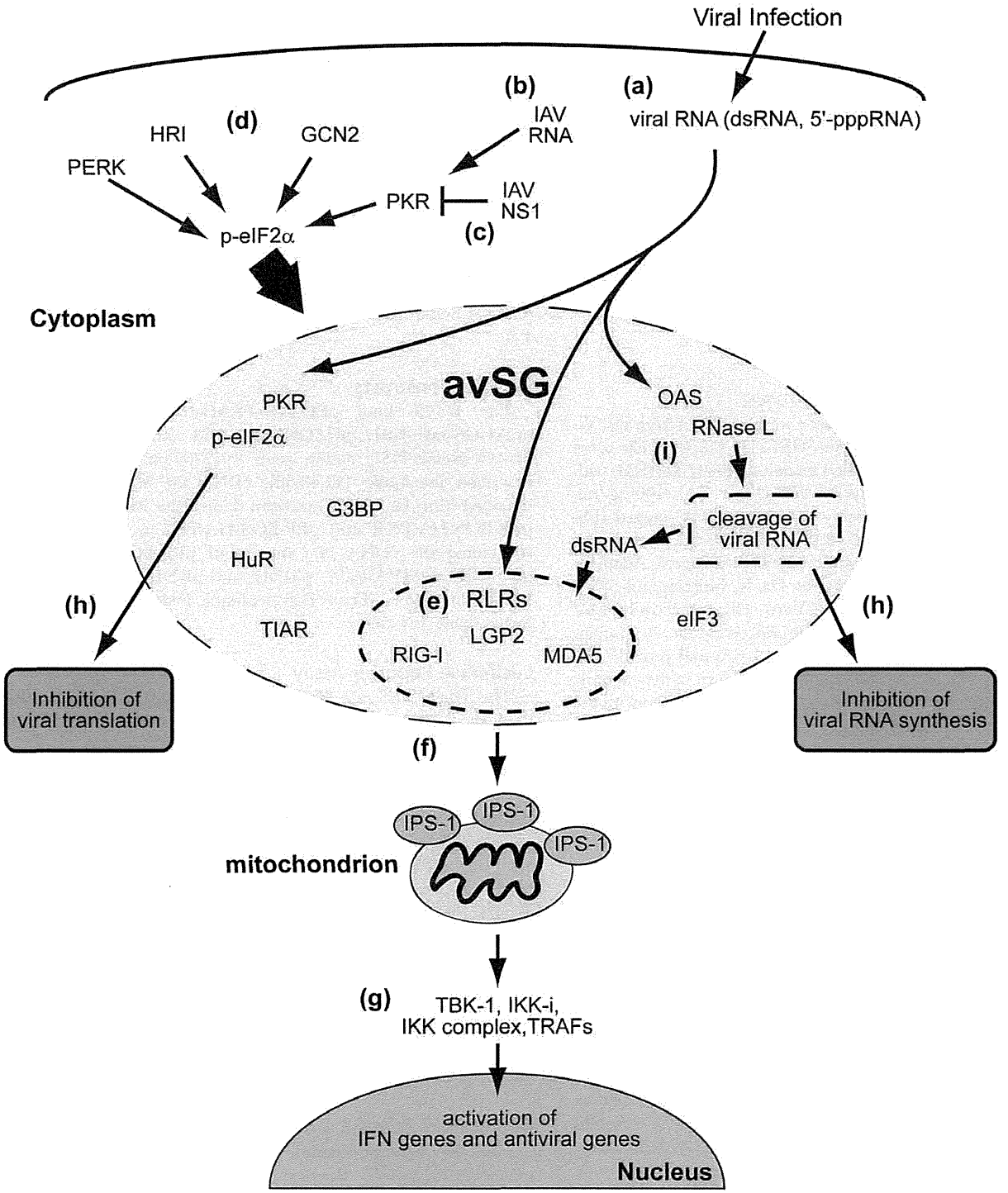

Figure 9. avSGs and innate antiviral responses. Viral infections generate RNA with non-self-signatures such as a 5′-tri-phosphate or double-stranded structure (**a**). In the case of IAVÄNS1, PKR is critical for the formation of avSGs (**b**). Wild-type IAV inhibits formation of avSGs by the actions of the NS1 protein (**c**). Some other viruses may activate different eIF2á kinases, such as GCN2, PERK, and HRI, to produce functional avSGs (**d**). avSGs are composed of SG markers and other RNA-binding proteins including RLRs, antiviral proteins (PKR, OAS, and RNase L) and viral RNA. Within avSGs, viral RNA could be sensed by RLRs to trigger antiviral signaling (**e**). Activated RLRs recruit mitochondrial IPS-1 via CARD-CARD interactions (**f**). IPS-1 serves as another platform for TRAFs and protein kinases, TBK-1, IKKi and IKK complex, to activate target genes (**g**). The antiviral proteins are activated by viral RNA to block viral RNA synthesis and translation (**h**). Moreover, OAS-RNase L system may produce dsRNA to amplify the RLR signaling (**i**).
doi:10.1371/journal.pone.0043031.g009

preventing PKR activation and phosphorylation eIF2á and the Vaccinia virus ÄE3L, lacking E3L genes, generated a granular-like structure distinguished from a granule termed antiviral granule (AVG) [47]. They also reported that MEFs lacking the AVG component TIA-1 exhibited increased Vaccinia viral replication, suggesting that AVG is critical for antiviral host responses. These

results strongly suggest that viruses acquire means to inhibit the formation of avSGs and subsequent activation of the IFN gene.

The canonical SG has been proposed as a storage compartment for translation-stalled host mRNA in response to various stresses and possible partner with another RNP complex, processing body, which is responsible for mRNA degradation [33]. Therefore, SG has been considered as a compartment for dynamic translational regulation upon environmental stress. Our findings discover a new role for newly identified avSG as a platform for interaction between viral RNA and host antiviral molecules to trigger a cascade of events leading to eradication of the virus. Although the difference between SG and avSG is not fully understood at this point, future research will delineate mechanism of their assembly and biological functions in stresses and immune responses.

Materials and Methods

Cell Culture, Transfection, and Viruses

MEFs from *pkr* +/+ and −/− mice were obtained from Dr. Yi-Li Yang [26]. HeLa, 293T, and HEC-1B [48,49] cells were maintained in Dulbecco's modified Eagle's medium (DMEM) with FBS and penicillin-streptomycin (100 U/ml and 100 μg/ml, respectively). HeLa cell line stably expressing FLAG-tagged IPS-1 was described previously [12]. 293T cells were transfected with FuGENE6 (Roche) or Lipofectamine 2000 (Invitrogen). Adenovirus type 12 (Ad12) dl203, provided by Dr. K. Shiroki, and SINV were propagated in 293T cells and Vero cells, respectively. IAV (A/PR/8/34 and ÄNS1), originally produced by Dr. A. Garcia-Sastre (Mount Sinai School of Medicine, USA) and provided by Dr. S. Akira (Osaka University, Japan), were grown in the allantoic cavities of 9-day-old embryonated eggs. Cells were treated with the culture medium ('mock-treated') or infected with IAV, IAVÄNS1, SINV, EMCV, or Ad12 dl203 in serum-free and antibiotic-free medium. After adsorption for 1 h at 37°C, the medium was changed and infection was continued for various periods in the presence of serum-containing DMEM. IAV genomic RNA was extracted from partially purified virus stock by TRIzol (Invitrogen) and 1.0 μg of viral RNA was transfected with Lipofectamine RNAi MAX (Invitrogen) in a 35 mm dish. PolyI:C was purchased from Amersham. Short polyI:C was prepared as described previously [27].

Immunoblotting, Antibodies and Reagents

The preparation of cell extracts and immunoblotting have already been described previously [5,50]. The polyclonal antibody used to detect human IRF-3 in native PAGE and anti-human and anti-mouse IRF-3 polyclonal antibodies for immunostaining were described previously [50]. The monoclonal antibody against Influenza NP (mAb61A5), which was generated by Dr. Y. Kikuchi (Iwaki Meisei University, Japan), was provided by Dr. F. Momose (Kitasato University, Japan) [51]. The monoclonal antibody against human OAS (6-1) was provided by Dr. Y. Sokawa (Kyoto Institute of Technology, Japan). The anti-human RIG-I, anti-human MDA5, and anti-human LGP2 antibodies were originally generated by immunizing rabbits with a synthetic peptide corresponding to amino acids 793–807 of human RIG-I, 145–160 of human MDA5, and 535–553 of human LGP2, respectively. As shown in Figure S1, knockdown of endogenous RIG-I by shRNAs specifically inhibit granule-like accumulation of RIG-I in immunostaining (Figure S1A) and appearance of band corresponding endogenous RIG-I in western blotting (Figure S1B), indicating high specificity of the anti-RIG-I antibody. Furthermore, a similar staining pattern was obtained with a monoclonal antibody for human RIG-I produced by Perseus Proteomics Inc, Japan. Other antibodies were obtained from the following sources: anti-G3BP (611126) from Transduction Laboratories™, anti-IRF-3 (CBX00167) from COSMO BIO, anti-PKR (sc-6282), anti-RNase L (sc-22870), anti-G3BP (sc-70283), anti-eIF3 (sc-16377), anti-c-myc (sc-40) and anti-TIAR (sc-1749) from Santa Cruz Biotechnology, anti-FLAG (M2) from Sigma, anti-phospho-PKR (pT446) (1120-1) from Epitomics, anti-actin (MAB1501R) from CHEMICON International, anti-PMP70 (ab3421) from Abcam, anti-HA-Tag (6E2) and anti-phospho-eIF2á (Ser51) (119A11) from Cell Signaling, and anti-HuR (RN004P, RIP-Certified antibody) and anti-â-actin (PM053) from MBL. Alexa 488-, 594-, and 633-conjugated anti-mouse, anti-rabbit, or anti-goat IgG antibodies purchased from Invitrogen were used as secondary antibodies. 0.5 mM Sodium arsenite (Sigma) was added to the cell culture for 1 h.

Plasmid Constructs

The p-125 Luc, pEF-BOS-FLAG-IPS-1, pCAGGS-myc, pCAGGS-myc-NS1, pCAGGS-myc-NS1 (amino acids 1–80), pCAGGS-myc-NS1 (amino acids 81–230) plasmids have been described previously [42,48,52]. cDNA for human PKR was obtained from Dr. A. Hovanessian (University Paris, France) and pEF-BOS-HA-PKR and pEF-BOS-HA-IPS1 were obtained by subcloning the cDNA into the vector pEF-BOS, respectively. pSUPER, pCMVÄR8.91, pMDG, and pRDI292 were provided by Dr. D. Trono (Ecole Polytechnique Federale de Lausanne, Switzerland) [53–56].

Luciferase Reporter Assay

The Dual-Luciferase Reporter Assay System (Promega) was used according to the manufacturer's instructions for luciferase assays. As an internal control, the *Renilla* Luciferase construct pRL-TK (Promega) was used.

Immunofluorescence Microscopy

Cells were fixed with 4% paraformaldehyde (PFA) for 20 min at 4°C, permeabilized with 0.05% Triton X-100 in PBS for 5 min at room temperature (RT), blocked with 5 mg/ml BSA in PBST (0.04% Tween20 in PBS) for 30 min, and incubated with relevant primary antibodies diluted in blocking buffer overnight at 4°C. The cells were then incubated with secondary antibodies for 1 h at RT. Nuclei were stained with 4.6-dimaidino-2-phenylinodole (DAPI) and analyzed with a confocal laser microscope, LSM 510-V4.2 (Carl Zeiss) or TCS-SP (Leica). The percentages of avSG-containing cells were calculated in more than 5 randomly chosen fields for each slide.

Quantitative Reverse Transcription-PCR

Total RNA was prepared with TRIzol reagent (Invitrogen), treated with DNase I (Roche Applied Science), and amplified by reverse transcription-PCR with the ABI PRISM 7700 sequence detection system (Applied Biosystems). TaqMan reverse transcription reagents (Applied Biosystems) were used for cDNA synthesis. We used commercial TaqMan Universal PCR Master Mix and TaqMan primer-probe sets (Applied Biosystems) for human and mouse IFN-â. As an internal control for the comparative threshold cycle methods, a primer-probe set for eukaryotic 18 s rRNA (Applied Biosystems) was used. The results were normalized to the abundance of internal control. For the detection of IAV RNA and glyceraldehyde-3-phophate dehydrogenase (GAPDH), we used specific primer sets and amplified with Ex Taq HS (Takara). IAV RNA: 5¢- ATTTGCAACACTACAGGGGC-3¢ (forward) and

5¢-GACTGACGAAAGGAATCCCA-3¢ (reverse). GAPDH mRNA:

5¢- GAGTCAACGGATTTGGTCGT-3¢ (forward) and

5¢- TTGATTTTGGAGGGATCTCG-3¢ (reverse).

Co-immunoprecipitation

The RIG-I antibody was cross-linked to Dynabeads protein G (Invitrogen) according to the manufacturer's protocol. Cell lysate was incubated with the anti-RIG-I antibody -Dynabeads for 120 min at RT. RIG-I-immunoprecipitated complexes were eluted by boiling in loading buffer and then processed for Western blotting.

RNA Interference

A lentiviral shRNA expression system was used. RIG-I shRNA#1 and RIG-I shRNA#2 were originally constructed. Oligonucleotides with the following sense and antisense sequences were used for the construction of the small hairpin RNA (shRNA)-encoding lentiviral vector. RIG-I shRNA#1; 5¢-GATCCCC-GAGGTGCAGTATATTCAGGTT CAAGAGACCTGAATA-TACTGCACCTCTTTTTGGAAA-3¢ (sense) and 5¢-AGCTT T TCCAAAAAGAGGTGCAGTATATTCAGGTCTCTT-GAACCTGAATATACTG CACCTCGGG-3¢ (antisense). RIG-I shRNA#2; 5¢-GATCCCCGAATTTAAAACCA GAAT-TATCTTCAAGAGAGATAATTCTGGTTT-TAAATTCTTTTTGGAAA-3¢ (sense) and 5¢-AGCTTTTC-CAAAAAGAATTTAAAACCAGAATTATCTCTC TTGAA-GATAATTCTGGTTTTAAATTCGGG-3¢ (antisense). The oligonucleotides described above were annealed and subcloned into the Bgl II-Hind III site of pSUPER. To construct the pLV-shRNA against RIG-I, the BamHI-SalI fragments excised from pSUPER-RIG-I#1 and pSUPER-RIG-I#2 were subcloned into the BamHI-SalI site of pRDI292. The recombinant lentiviruses were generated by transfection of the empty lentiviral vector, or respective shRNA construct together with the packaging construct pCMVÄR8.91 and the envelop plasmid pMDG. At 48 h after, the culture supernatant was collected and the medium filtered with a 0.45-μm filter was transferred, to HeLa cells. After 72 h, the cells were selected with medium containing 2 μg/ml of Puromycin (Sigma). The siRNA negative control and siRNAs targeting PKR and G3BP were purchased from Invitrogen. Each siRNA was transfected with Lipofectamine RNAi MAX (Invitrogen) according to the manufacturer's instructions. At 48 h post-transfection, cells were harvested, infected with IAVÄNS1, and then subjected to Real Time PCR, immunofluorescence assays, or SDS-PAGE followed by immunoblotting.

Fluorescence in situ Hybridization (FISH) Assay

FISH assays have been described previously [57]. Briefly, after the immunofluorescence assays, cells were fixed in 4%PFA for 10 min and permeablized on ice with 0.5% Triton X-100 in PBS for 5 min. After deproteinization by Proteinase K, cells were re-fixed in 4% PFA for 10 min and then subjected to stepwise dehydration in ethanol. The dried coverslips were incubated with a biotin-labeled RNA probe for 12 h at 37°C. After hybridization, cells were washed and incubated with avidin-FITC for 30 min at 37°C. Nuclei were stained with TO-PRO-3 and examined by confocal laser-scanning microscope.

Enzyme-linked Immunosorbent Assay (ELISA)

Culture supernatants were collected and subjected to ELISA with mouse IFN-â kit (PBL Interferon Source) according to the manufacturers' instructions.

Supporting Information

Figure S1 Anti-RIG-I antibody specifically recognizes endogenous human RIG-I. HeLa cells were infected with control lentivirus or two lentiviruses encoding different RIG-I-specific shRNAs (#1 and #2) for 72 h. **(A)** The cells were treated with $NaAsO_2$ for 1 h and stained for RIG-I and G3BP. $NaAsO_2$ induces speckle-like localization of RIG-I and G3BP. **(B)** The cells were treated with human IFN-â for 12 h. Cell extracts were prepared and subjected to SDS-PAGE, and immunoblotted using antibodies against RIG-I, MDA5, and â-actin. The RIG-I signals were diminished by knockdown of RIG-I.
(TIF)

Figure S2 N-terminal region of NS1 is sufficient to block RIG-I aggregation and antiviral signals. (A) 293T cells were transfected with empty vector (empty), myc-tagged NS1 (myc-NS1 (Full)), N-terminal NS1 (1–80), or C-terminal NS1 (81–230) for 48 h. The cells were mock-treated (mock) or infected with IAVÄNS1 for 9 h and stained for RIG-I and NS1 (myc). The percentage of cells with IAVÄNS1-induced RIG-I speckle was 0.0%, 2.3%, 43.1%, for NS1, NS1 (1–80), and NS1 (81–230)-expressing cells, respectively. **(B)** 293T cells were transiently transfected with reporter plasmids containing natural IFN-â promoter together with the indicated NS1-expressing vectors. Transfected cells were mock-treated or infected with IAVÄNS1 for 12 h and subjected to the Dual-Luciferase assay. Data are presented as the mean standard ± error of the mean (SEM).
(TIF)

Figure S3 Localization of Viral RNA in IAV-infected cells. (A and B) HeLa cells were mock-treated or infected with IAV for 12 h. Viral RNA (vRNA) was detected by the FISH method using an RNA probe complementary to the segment 1 of IAV and NP **(A)** and RIG-I **(B)** were detected using anti-NP and anti-RIG-I antibodies. TO-PRO-3 was used for staining of nuclear DNA (DNA). Viral RNA and NP did not form foci.
(TIF)

Figure S4 IPS-1 was accumulated in close proximity to the RIG-I foci. HeLa cells stably expressing FLAG-tagged IPS-1 were mock-treated or infected with IAV or IAVÄNS1 for 10 h. The cells were stained with anti-FLAG and anti-RIG-I antibodies and DAPI. The merged images of FLAG and RIG-I are enlarged in the bottom panel. The white arrowheads indicate RIG-I/IPS-1 contacts. These contacts were observed in 74.2% and 1.8% of IAVÄNS1- and IAV-infected cells, respectively.
(TIF)

Figure S5 avSG formation is not a consequence of IFN gene activation. (A) 293T cells were transfected with empty vector or the expression vector for IPS-1 (HA-IPS-1) for 24 h. Cells were stained for IRF-3, HA-tag and TIAR. Nuclear IRF-3 was observed in almost all of the IPS-1-expressing cells (95.5%), however these cells exhibited little foci of TIAR (3.0%). **(B)** HEC-1B cells deficient for type I IFN receptor were mock-treated, infected with IAVÄNS1 for 9 h, or treated with $NaAsO_2$ for 1 h as indicated. Cells were stained for RIG-I and G3BP. SGs and avSGs were observed in HEC-1B cells (% colocalization 98.4% and 92.9% for IAVÄNS1 and $NaAsO_2$, respectively). The zoomed images correspond to the boxed regions. **(C)** HeLa cells were mock-treated or infected with SINV, EMCV, or Ad12 dl203 for 9 h, fixed, and stained for RIG-I and G3BP as indicated (% colocalization: 99.2%, 98.4%, and 98.2%, respectively). The zoomed images correspond to the boxed regions.
(TIF)

Figure S6 IAV-induced formation of avSGs was inhibited in PKR knockdown cells. **(A–E)** HeLa cells were transfected with control siRNA (N.C) or siRNA targeting three independent parts of human PKR mRNA (#1 3). **(A)** At 48 h after transfection, cells were harvested and PKR and actin were detected by Western blotting. **(B–E)** At 48 h after transfection, cells were mock-treated (open bar) or infected with IAVÄNS1 (filled bar) for 9 h. The level of IFN-â mRNA was determined by qPCR **(B)**. Immunostaining of HeLa cells transfected with control (N.C) or PKR-targeted (PKR) siRNA after mock-treatment or infection with IAVÄNS1 **(C)**. Cells were also examined by staining for foci of RIG-I **(D)**, TIAR **(E)** after 12 h infection. Percentages of cells containing the respective foci are indicated. Data are presented as the mean standard ± error of the mean (SEM).
(TIF)

Figure S7 Total RNA from IAV-infected cells but not uninfected cells induces avSG formation and IFN-â gene activation. **(A and B)** Wild-type MEF were mock-treated (no RNA) or transfected with total RNA extracted from uninfected MEFs (MEF RNA) or from IAV-infected cells for 12 h (IAV infected MEF RNA). The cells were stained for RIG-I and G3BP (% avSG formation 0.0%, 4.0%, and 21.4% for no RNA, MEF RNA, and IAV infected MEF RNA, respectively) **(A)**. The zoomed images correspond to the boxed regions. Endogenous IFN-â mRNA levels were determined by qPCR **(B)**. Data are presented as the mean standard ± error of the mean (SEM).
(TIF)

Acknowledgments

We thank R. Kageyama for making their confocal microscope available for this study, F. Momose and Y. Kikuchi for the anti-IAV NP antibody, and Y. Sokawa for the anti-OAS antibody.

Author Contributions

Conceived and designed the experiments: KO MY TF. Performed the experiments: KO MJ JY RN SM AT AK SO TM. Analyzed the data: KO KN HN MY TF. Contributed reagents/materials/analysis tools: SS. Wrote the paper: KO MY TF.

References

1. Samuel CE (2001) Antiviral actions of interferons. Clin Microbiol Rev 14: 778–809, table of contents.
2. Witte K, Witte E, Sabat R, Wolk K (2010) IL-28A, IL-28B, and IL-29: promising cytokines with type I interferon-like properties. Cytokine Growth Factor Rev 21: 237–251.
3. Gale M Jr, Katze MG (1998) Molecular mechanisms of interferon resistance mediated by viral-directed inhibition of PKR, the interferon-induced protein kinase. Pharmacol Ther 78: 29–46.
4. Rubinstein S, Familletti PC, Pestka S (1981) Convenient assay for interferons. J Virol 37: 755–758.
5. Yoneyama M, Kikuchi M, Natsukawa T, Shinobu N, Imaizumi T, et al. (2004) The RNA helicase RIG-I has an essential function in double-stranded RNA-induced innate antiviral responses. Nat Immunol 5: 730–737.
6. Kato H, Takeuchi O, Sato S, Yoneyama M, Yamamoto M, et al. (2006) Differential roles of MDA5 and RIG-I helicases in the recognition of RNA viruses. Nature 441: 101–105.
7. Yoneyama M, Kikuchi M, Matsumoto K, Imaizumi T, Miyagishi M, et al. (2005) Shared and unique functions of the DExD/H-box helicases RIG-I, MDA5, and LGP2 in antiviral innate immunity. J Immunol 175: 2851–2858.
8. Hornung V, Ellegast J, Kim S, Brzozka K, Jung A, et al. (2006) 5′-Triphosphate RNA is the ligand for RIG-I. Science 314: 994–997.
9. Pichlmair A, Schulz O, Tan CP, Naslund TI, Liljestrom P, et al. (2006) RIG-I-mediated antiviral responses to single-stranded RNA bearing 5′-phosphates. Science 314: 997–1001.
10. Rasmussen SB, Jensen SB, Nielsen C, Quartin E, Kato H, et al. (2009) Herpes simplex virus infection is sensed by both Toll-like receptors and retinoic acid-inducible gene- like receptors, which synergize to induce type I interferon production. J Gen Virol 90: 74–78.
11. Samanta M, Iwakiri D, Kanda T, Imaizumi T, Takada K (2006) EB virus-encoded RNAs are recognized by RIG-I and activate signaling to induce type I IFN. EMBO J 25: 4207–4214.
12. Onoguchi K, Onomoto K, Takamatsu S, Jogi M, Takemura A, et al. (2010) Virus-infection or 5′ppp-RNA activates antiviral signal through redistribution of IPS-1 mediated by MFN1. PLoS Pathog 6: e1001012.
13. Hale BG, Randall RE, Ortin J, Jackson D (2008) The multifunctional NS1 protein of influenza A viruses. J Gen Virol 89: 2359–2376.
14. Portela A, Digard P (2002) The influenza virus nucleoprotein: a multifunctional RNA-binding protein pivotal to virus replication. J Gen Virol 83: 723–734.
15. Buchan JR, Parker R (2009) Eukaryotic stress granules: the ins and outs of translation. Mol Cell 36: 932–941.
16. Hou F, Sun L, Zheng H, Skaug B, Jiang QX, et al. (2011) MAVS Forms Functional Prion-like Aggregates to Activate and Propagate Antiviral Innate Immune Response. Cell 146: 448–461.
17. Xu LG, Wang YY, Han KJ, Li LY, Zhai Z, et al. (2005) VISA is an adapter protein required for virus-triggered IFN-beta signaling. Mol Cell 19: 727–740.
18. Seth RB, Sun L, Ea CK, Chen ZJ (2005) Identification and characterization of MAVS, a mitochondrial antiviral signaling protein that activates NF-kappaB and IRF 3. Cell 122: 669–682.
19. Kawai T, Takahashi K, Sato S, Coban C, Kumar H, et al. (2005) IPS-1, an adaptor triggering RIG-I- and Mda5-mediated type I interferon induction. Nat Immunol 6: 981–988.
20. Meylan E, Curran J, Hofmann K, Moradpour D, Binder M, et al. (2005) Cardif is an adaptor protein in the RIG-I antiviral pathway and is targeted by hepatitis C virus. Nature 437: 1167–1172.
21. Dixit E, Boulant S, Zhang Y, Lee AS, Odendall C, et al. (2010) Peroxisomes are signaling platforms for antiviral innate immunity. Cell 141: 668–681.
22. White JP, Cardenas AM, Marissen WE, Lloyd RE (2007) Inhibition of cytoplasmic mRNA stress granule formation by a viral proteinase. Cell Host Microbe 2: 295–305.
23. Nallagatla SR, Hwang J, Toroney R, Zheng X, Cameron CE, et al. (2007) 5′-triphosphate-dependent activation of PKR by RNAs with short stem-loops. Science 318: 1455–1458.
24. Baum A, Sachidanandam R, Garcia-Sastre A (2010) Preference of RIG-I for short viral RNA molecules in infected cells revealed by next-generation sequencing. Proc Natl Acad Sci U S A 107: 16303–16308.
25. Rehwinkel J, Tan CP, Goubau D, Schulz O, Pichlmair A, et al. (2010) RIG-I detects viral genomic RNA during negative-strand RNA virus infection. Cell 140: 397–408.
26. Yang YL, Reis LF, Pavlovic J, Aguzzi A, Schafer R, et al. (1995) Deficient signaling in mice devoid of double-stranded RNA-dependent protein kinase. EMBO J 14: 6095–6106.
27. Kato H, Takeuchi O, Mikamo-Satoh E, Hirai R, Kawai T, et al. (2008) Length-dependent recognition of double-stranded ribonucleic acids by retinoic acid-inducible gene-I and melanoma differentiation-associated gene 5. J Exp Med 205: 1601–1610.
28. Yoneyama M, Fujita T (2010) Recognition of viral nucleic acids in innate immunity. Rev Med Virol 20: 4–22.
29. Malathi K, Dong B, Gale M Jr, Silverman RH (2007) Small self-RNA generated by RNase L amplifies antiviral innate immunity. Nature 448: 816–819.
30. Berlanga JJ, Ventoso I, Harding HP, Deng J, Ron D, et al. (2006) Antiviral effect of the mammalian translation initiation factor 2alpha kinase GCN2 against RNA viruses. EMBO J 25: 1730–1740.
31. Ouda R, Onomoto K, Takahasi K, Edwards MR, Kato H, et al. (2011) Retinoic acid-inducible gene I-inducible miR-23b inhibits infections by minor group rhinoviruses through down-regulation of the very low density lipoprotein receptor. J Biol Chem 286: 26210–26219.
32. Saito T, Hirai R, Loo YM, Owen D, Johnson CL, et al. (2007) Regulation of innate antiviral defenses through a shared repressor domain in RIG-I and LGP2. Proc Natl Acad Sci U S A 104: 582–587.
33. Kedersha N, Anderson P (2007) Mammalian stress granules and processing bodies. Methods Enzymol 431: 61–81.
34. Diebold SS, Montoya M, Unger H, Alexopoulou L, Roy P, et al. (2003) Viral infection switches non-plasmacytoid dendritic cells into high interferon producers. Nature 424: 324–328.
35. Gilfoy FD, Mason PW (2007) West Nile virus-induced interferon production is mediated by the double-stranded RNA-dependent protein kinase PKR. J Virol 81: 11148–11158.
36. McAllister CS, Samuel CE (2009) The RNA-activated protein kinase enhances the induction of interferon-beta and apoptosis mediated by cytoplasmic RNA sensors. J Biol Chem 284: 1644–1651.
37. Carpentier PA, Williams BR, Miller SD (2007) Distinct roles of protein kinase R and toll-like receptor 3 in the activation of astrocytes by viral stimuli. Glia 55: 239–252.
38. Barry G, Breakwell L, Fragkoudis R, Attarzadeh-Yazdi G, Rodriguez-Andres J, et al. (2009) PKR acts early in infection to suppress Semliki Forest virus production and strongly enhances the type I interferon response. J Gen Virol 90: 1382–1391.

39. Schulz O, Pichlmair A, Rehwinkel J, Rogers NC, Scheuner D, et al. (2010) Protein kinase R contributes to immunity against specific viruses by regulating interferon mRNA integrity. Cell Host Microbe 7: 354–361.
40. Min JY, Li S, Sen GC, Krug RM (2007) A site on the influenza A virus NS1 protein mediates both inhibition of PKR activation and temporal regulation of viral RNA synthesis. Virology 363: 236–243.
41. Khaperskyy DA, Hatchette TF, McCormick C (2011) Influenza A virus inhibits cytoplasmic stress granule formation. FASEB J.
42. Guo Z, Chen LM, Zeng H, Gomez JA, Plowden J, et al. (2007) NS1 protein of influenza A virus inhibits the function of intracytoplasmic pathogen sensor, RIG-I. Am J Respir Cell Mol Biol 36: 263–269.
43. Mibayashi M, Martinez-Sobrido L, Loo YM, Cardenas WB, Gale M Jr, et al. (2007) Inhibition of retinoic acid-inducible gene I-mediated induction of beta interferon by the NS1 protein of influenza A virus. J Virol 81: 514–524.
44. Gack MU, Albrecht RA, Urano T, Inn KS, Huang IC, et al. (2009) Influenza A virus NS1 targets the ubiquitin ligase TRIM25 to evade recognition by the host viral RNA sensor RIG-I. Cell Host Microbe 5: 439–449.
45. Li W, Li Y, Kedersha N, Anderson P, Emara M, et al. (2002) Cell proteins TIA-1 and TIAR interact with the 3′ stem-loop of the West Nile virus complementary minus-strand RNA and facilitate virus replication. J Virol 76: 11989–12000.
46. Iseni F, Garcin D, Nishio M, Kedersha N, Anderson P, et al. (2002) Sendai virus trailer RNA binds TIAR, a cellular protein involved in virus-induced apoptosis. EMBO J 21: 5141–5150.
47. Simpson-Holley M, Kedersha N, Dower K, Rubins KH, Anderson P, et al. (2010) Formation of antiviral cytoplasmic granules during orthopoxvirus infection. J Virol 85: 1581–1593.
48. Yoneyama M, Suhara W, Fukuhara Y, Fukuda M, Nishida E, et al. (1998) Direct triggering of the type I interferon system by virus infection: activation of a transcription factor complex containing IRF-3 and CBP/p300. EMBO J 17: 1087–1095.
49. Daly C, Reich NC (1993) Double-stranded RNA activates novel factors that bind to the interferon-stimulated response element. Mol Cell Biol 13: 3756–3764.
50. Iwamura T, Yoneyama M, Yamaguchi K, Suhara W, Mori W, et al. (2001) Induction of IRF-3/−7 kinase and NF-kappaB in response to double-stranded RNA and virus infection: common and unique pathways. Genes Cells 6: 375–388.
51. Momose F, Kikuchi Y, Komase K, Morikawa Y (2007) Visualization of microtubule-mediated transport of influenza viral progeny ribonucleoprotein. Microbes Infect 9: 1422–1433.
52. Onoguchi K, Yoneyama M, Takemura A, Akira S, Taniguchi T, et al. (2007) Viral infections activate types I and III interferon genes through a common mechanism. J Biol Chem 282: 7576–7581.
53. Brummelkamp TR, Bernards R, Agami R (2002) A system for stable expression of short interfering RNAs in mammalian cells. Science 296: 550–553.
54. Naldini L, Blomer U, Gallay P, Ory D, Mulligan R, et al. (1996) In vivo gene delivery and stable transduction of nondividing cells by a lentiviral vector. Science 272: 263–267.
55. Zufferey R, Nagy D, Mandel RJ, Naldini L, Trono D (1997) Multiply attenuated lentiviral vector achieves efficient gene delivery in vivo. Nat Biotechnol 15: 871–875.
56. Bridge AJ, Pebernard S, Ducraux A, Nicoulaz AL, Iggo R (2003) Induction of an interferon response by RNAi vectors in mammalian cells. Nat Genet 34: 263–264.
57. Jo S, Kawaguchi A, Takizawa N, Morikawa Y, Momose F, et al. (2010) Involvement of vesicular trafficking system in membrane targeting of the progeny influenza virus genome. Microbes Infect 12: 1079–1084.

Journal of Clinical Laboratory Analysis 26: 174–183 (2012)

New Sandwich-Type Enzyme-Linked Immunosorbent Assay for Human MxA Protein in a Whole Blood Using Monoclonal Antibodies Against GTP-Binding Domain for Recognition of Viral Infection

Mizuho Kawamura,[1] Akira Kusano,[2] Akiko Furuya,[2] Nobuo Hanai,[2] Hideki Tanigaki,[1] Akihito Tomita,[1] Akira Horiguchi,[3] Kyosuke Nagata,[4] Toshiko Itazawa,[5] Yuichi Adachi,[5] Yoshie Okabe,[5] Toshio Miyawaki,[5] and Hiroaki Kohno[1]*

[1]Fuji Research Laboratories, Kyowa Medex Co., Ltd., Shizuoka, Japan
[2]Tokyo Research Park, Kyowa Hakko Kirin Co., Ltd., Tokyo, Japan
[3]Department of Research and Development, Kyowa Medex Co., Ltd., Tokyo, Japan
[4]Department of Infection Biology, Faculty of Medicine, University of Tsukuba, Tsukuba, Japan
[5]Department of Pediatrics, Faculty of Medicine, University of Toyama, Toyama, Japan

Objectives: To develop a clinically significan and practical enzyme-linked immunosorbent assay (ELISA) for the detection of MxA protein in human whole blood, a biological marker of viral infection. *Design and Methods:* A sandwich ELISA suitable for the measurement of human MxA protein in whole blood was developed using mouse monoclonal antibodies (mAbs) raised against the GTP-binding domain of human MxA protein. Prior to the assay, the whole blood sample was treated with special buffer to extract the MxA protein, improve its stability, and avoid interference from hemoglobin. *Results:* This ELISA meets all the requirements for use in routine clinical assays, especially in terms of sensitivity (detection limit: 1.3 ng/ml whole blood), accuracy (recovery: 93.0–100.0%), and rapidity (<1.5 h). The present ELISA had a sensitivity of100% and a specificit of 100% for viral infection when compared to samples from healthy control and 87.1% and 90.9% when compared to samples from the bacterial infection group. *Conclusion:* We have developed a new ELISA for measuring MxA protein in human whole blood using mAbs specifi for the GTP-binding domain of MxA. This ELISA has analytical performance enough for routine clinical assay and can be used in detecting the possibility of viral infection. J. Clin. Lab. Anal. 26:174–183, 2012.

Key words: bacterial infection; interferon α, high sensitivity; high stability; rapid assay

INTRODUCTION

Interferons are produced in response to viral infections and contribute to host defense by establishing an antiviral state in target cells (1,2). Directly measuring the interferon levels in plasma is technically difficult since interferon is rapidly turned over in vivo (3). Furthermore, the circulating level of interferon does not reflect the biologically active interferon effects on target cells (2,4).

The antiviral activity of the interferon is mediated by the induction of unique proteins and more than 30 different intracellular proteins are known to be induced by interferon (5). By measuring interferon-induced proteins, the presence of biologically active interferons can be detected more consistently (6). Among the interferon-induced proteins, MxA protein is remarkable for its high levels of expression that may reach 1% of the total cytosolic protein (7) and that can be specifically induced in a dose-dependent manner by interferons both in vivo and in vitro (7, 8). MxA protein is rapidly induced after interferon-treatment (1–2 h), detectable within 2–4 h after

*Correspondence to: Hiroaki Kohno, Fuji Research Laboratories, Kyowa Medex Co., Ltd., 600-1 Minami-isshiki, Nagaizumi-cho Suntoh-gun, Shizuoka Pref. 411-0932, Japan. E-mail: hiroaki.kohno@kyowa-kirin.co.jp

Received 7 August 2011; Accepted 24 February 2012
DOI 10.1002/jcla.21507
Published online in Wiley Online Library (wileyonlinelibrary.com).

interferon exposure, both in vitro and in vivo, and reaches a maximum level within 36 h (7–10). Moreover, cellular induction of MxA protein is not subject to feedback inhibition (8). Since interferons are the sole inducers of MxA protein (11), levels of MxA protein reflect the biologically active interferon present during host cell defense mechanisms. Therefore, elevated levels of MxA protein could be an indicator of endogenous interferon production mediated by an unknown viral activation (4) and so, the MxA protein levels could be used as a general marker of viral infection. It has been reported that MxA protein expression in peripheral blood mononuclear cells is a highly specific and reliable marker for interferon bioactivity (12) and that elevated leukocyte MxA protein levels reflect endogenous interferon production (13). Accordingly, the rapid determination of MxA protein from patient samples could be considered a useful test for the diagnosis of viral disease (14, 15).

Recent advances in the understanding of the structure and function of human MxA protein have revealed the presence of a GTP-binding domain and GTPase activity, which are now regarded as important factors in relation to its antiviral activity against a wide variety of viruses (16–20). Detailed elucidation of the relationship between the structure and function of MxA protein may make the accurate diagnosis of viral infectious conditions possible.

Here, we report the development of a clinically useful enzyme-linked immunosorbent assay (ELISA) for the detection of human MxA protein in whole blood, using mouse mAb that recognize a GTP-binding domain, which meet the requirements for a routine clinical assay.

MATERIALS, SAMPLES, AND METHODS

Materials and Chemicals

Reagents were obtained from the following sources: bovine serum albumin (BSA) (Miles, Inc., Kankakee, IL); 3,3′,5,5′-tetramethylbenzidine (TMBZ) solution (TMBlue, TSI Co., Milford, MA); oleamide diethanolamide (NOF Corporation, Tokyo, Japan), N-succinimidyl-6-maleimidohexanoate and 3-((3-Cholamidopropyl)dimethylammonio] propanesulfonate) (Dojindo Laboratories, Kumamoto, Japan); horseradish peroxidase (HRP) (Toyobo Co., Ltd., Osaka, Japan); BLOCK ACE® (DS pharma Biomedical Co., Ltd., Osaka, Japan); all other reagents were of analytical grade.

Clinical Samples

Whole blood samples from children who visited the outpatient clinic of Toyama University Hospital (Toyama, Japan) for acute onset fever were collected. Seventeen healthy children who had been without symptoms of infectious diseases during the previous two weeks served as controls. The study was conducted according to the ethical standards of the University of Toyama, which require informed consent from the parents of each subject.

Children with acute onset fever were subdivided into three groups according to the final diagnoses: (1) etiologically diagnosed viral infection, (2) clinically diagnosed viral infection, and (3) bacterial infection. Individuals with etiologically diagnosed viral infection were identified by positive results using the following virus-detection kits: Adenovirus GSA (Meridian Bioscience, Cincinnati, OH) for adenovirus, ROTA-ADENO DRY (Orion Diagnostica, Espoo, Finland) for rotavirus, Capilia Flu A, B (Nippon Becton Dickinson, Tokyo, Japan) for influenza viruses, and Directigen RSV (Becton Dickinson, Cockeyville, MD) for respiratory syncytial virus. Children with mild symptoms of upper respiratory infection or gastroenteritis were classified into the clinically diagnosed viral infection group. Their symptoms resolved spontaneously even though antibiotics were not used. Bacterial infections were diagnosed based on positive culture results and all the child patients with bacterial infections were treated successfully with antibiotics.

Whole blood samples were freshly prepared from EDTA anticoagulated blood. When whole blood was used for the ELISA, the sample was diluted immediately with the dilution buffer (0.1 mol/l Tris-HCl buffer [pH8.5] containing 2.5% [w/v] 3-[(3-Cholamidopropyl) dimethylammonio] propanesulfonate, 1.2% [w/v] oleamide diethanolamide, 0.1 mol/l NaCl, 4.0% [w/v] BLOCK ACE®, 0.1% [w/v] BSA, and 0.1% [w/v] NaN_3), stored at 4°C and was measured within 24 h after the collection. When the sample was stored for a long time, the diluted sample was stored at –80°C and was thawed just before ELISA assay.

Serum samples were prepared from blood allowed to clot at 37°C for 30 min, by centrifugation at 3,000 rpm for 10 min.

Preparation of MxA Protein

An expression vector pET-14b (Merck Biosciences, Darmstadt, Germany) containing full-length MxA protein-encoding cDNA was introduced into *Escherichia coli (E. coli)* cells (21), and were cultured at 37 °C for 4 h in 200 ml of LB medium containing 50 μg/ml of ampicillin, followed by the addition of 0.4 mmol/l of isopropylthiogalactoside and subsequently cultured at 37°C for 2 h.

E. coli was collected from 200 ml of the cultured broth by centrifugation at 3,000 rpm for 15 min, washed with phosphate-buffered saline (PBS), and was suspended in 20 mmol/l Tris-HCl buffer (pH7.9) containing 5 mmol/l imidazole and 0.5 mol/l NaCl, and then lysed by

ultrasonic treatment. After the suspension was centrifuged, the supernatant was discarded, and the residue was added to the binding buffer (20 mmol/l Tris-HCl buffer (pH7.9) containing 6 mol/l urea, 5 mmol/l imidazole, and 0.5 mol/l NaCl) and Ni-NTA His-Bind resin (EMD Bioscience, Inc., Milwaukee, WI) to purify full-length human MxA protein with a N-terminal His (6) tag from the *E. coli* inclusion bodies. The suspension was mixed by gentle rolling at 4°C for 2 h to bind MxA protein on the resin and the resin was recovered by centrifuge. The recovered resin was washed with the binding buffer and was eluted using 20 mmol/ml Tris-HCl buffer (pH7.9) containing 6 mol/l urea, 1 mol/l imidazole, and 0.5 mol/l NaCl to produce crude MxA protein. Using this method, 1.4 mg of MxA protein was recovered from 250 ml of the *E. coli* culture broth.

Immunization, Cell Fusion, and Cloning

BALB/C mice (six weeks old, male) were immunized with the recombinant human MxA protein. The monoclonal hybridoma cells were made by fusion with spleen cells derived from the immunized mouse and 2×10^7 P3×63-Ag.8.U1 cells, as described previously (22). Cell culture supernatants were tested for antibody activity by ELISA using a MxA protein-coated plate as described previously (22). Cells from positive wells were further selected on the basis of specificity and subclass, and were cloned twice by limiting dilution. Stable hybridoma clones were propagated as ascites tumors in BALB/C mice. Antibodies from monoclonal hybridoma cells were purified from the ascites by affinity chromatography using Protein-A Sepharose fast flow (GE healthscience Japan, Tokyo, Japan) according to the manufacturer's instructions.

The subclass of the monoclonal antibody was determined by a Zymed mouse mAb isotyping kit (Zymed Laboratories, Inc., San Francisco, CA). The dissociation constant of the antibody was determined by the method of Djavadi-Ohaniance et al. (23).

Western Blotting

One microgram of MxA protein derived from *E. coli* was fractionated by sodium dodecyl sulfate-polyacrylamide gel electrophoresis (SDS-PAGE) and then blotted on a polyvinylidene difluoride (PVDF) membrane. After blocking with a BSA solution, the membrane was incubated with 10 μg/ml of each of the purified anti-human MxA protein mAb for 2 h at room temperature. After thorough washing with PBS containing 0.1% (w/v) Tween 20, a HRP-labeled anti-mouse immunoglobulin antibody (DAKO Japan, Kyoto, Japan) was incubated at room temperature for 1 h. After thorough washing, color development was performed using the HAP-Color Development Reagent substrate solution (DAKO Japan).

Immnocytostaining

A suspension of human glioma T98G (ATCC CRL 1690) cells was dispensed in 500 μl portions to separate wells of an eight-well chamber slide (2×10^4 cells/well), stimulated with interferon α (1,000 U/ml) and cultured at 37°C. After washing with PBS, 500 μl of freshly prepared 4% (v/v) paraformaldehyde was added into each well and the cells were fixed at room temperature for 30 min.

The fixed cells were treated with 0.2% (v/v) Triton X-100 for 5 min to permeablize the cell membrane, incubated with 10% (v/v) normal horse serum for 30 min for blocking, and then with 10 μg/ml of each of the purified anti-human MxA protein mAb for 30 min at room temperature. After washing with PBS, 200 μl of fluorescein isothiocyanate (FITC)-labeled anti-mouse immunoglobulin antibody (Wako Pure Chemical Industries, Osaka, Japan) was added into each well at room temperature for 30 min in the dark. After thorough washing with PBS, the cells were sealed with glycerol on a glass slide and observed under a fluorescence microscope.

T98G infected with influenza virus were obtained from the Tokyo Institute of Technology and cultured at 37°C. The T98G were fixed with 4% (v/v) paraformaldehyde and were used for immunocytostaining using the same method as described above.

Determination of the mAb-Binding Domain

The MxA protein-encoding DNA was digested with restriction enzymes BstXI, PstI, NaeI, and BamHI following established procedures, and was subjected to in vitro transcription in the presence of T7 RNA polymerase to synthesize several mRNA samples having different lengths. Next, in vitro translation was carried out using these mRNA samples in the presence of ^{35}S-methionine to synthesize ^{35}S-methionine-labeled protein fragments that were successively shortened from the C-terminal end. The in vitro translation was carried out using reticulocyte lysate (#L416A, E. Y. Labo Inc., San mateo, CA) in accordance with the manufactured instruction manual. As a result, labeled protein fragments corresponding to amino acids 10–662, amino acids 10–468, amino acids 10–297 and amino acids 10–220, were synthesized. Each of these labeled protein fragments were allowed to react with each of the anti-human MxA protein mAb in a reaction buffer (50 mmol/l Tris-HCl buffer (pH 8.0) containing 1% (v/v) NP-40 and 0.2% (w/v) BSA) at 4°C for 1 h. The reaction solution was mixed with 40 μl of secondary antibody-labeled beads (AG-005, E. Y. Labo Inc.) and the reaction incubated at 4°C for 1 h with shaking for immunoprecipitation. The reaction mixture was subjected to

centrifugation at 10,000 × *g* at 4°C for 15 s and the precipitate obtained was separated by SDS-PAGE and the molecular weight of the precipitated protein was determined by autoradiography.

ELISA System

Sensitization of plates

KM1135-coated polystyrene 96-well microtiter plates (Maxisorp Immunoplates, NUNC, Rosklide, Denmark) were prepared as described previously (24). The plates were sealed in an aluminum-coated pack with a drying agent (Hi-sheet dry, Marutani chemical Plant & Engineering Co., Ltd., Tokyo, Japan) and stored at 4°C until use. Under these storage conditions, the sensitized plates were stable for at least 1 year.

Antibody-HRP conjugate

The KM1124-HRP conjugate was prepared as described previously (24). The average number of HRP molecules introduced per IgG molecule was 4.3.

The conjugate produced was diluted to 50 ng/ml with 50 mmol/l Bis-Tris buffer (pH 7.0) containing 0.1% (w/v) BSA, 50 mmol/l NaCl, 0.01% (w/v) 4-aminoantipyrine, 0.1% (v/v) polyoxyethylene polyoxypropylene glycol, 0.035% (v/v) Proclin 300® (Sigma-Aldrich Japan Co, Tokyo, Japan), and 100 mg/l mouse IgG (Roche Diagnostics GmbH, Mannheim, Germany), divided into 11 ml each in clear bottles and stored at 4°C until use. Under these storage conditions, the conjugate was stable for at least 1 year.

Standard preparation

For the standard in the ELISA, a recombinant MxA protein was prepared from *E. coli* cells transformed with an expression vector containing a MxA protein-encoding cDNA as described above. The recombinant MxA protein was furthermore purified by gel filtration column chromatography using Superose 12HR10/30 (GE healthscience Japan) eluted with 20 mmol/ml Tris-HCl buffer (pH7.9) containing 6 mol/l urea, 0.5 mmol/l imidazole, 0.1 mmol/l dithiothreitol, and 0.5 mol/l NaCl at 0.5 ml/min. The highly purified MxA protein was confirmed to be monomeric and homogeneous by high performance liquid chromatography (HPLC) and SDS-PAGE, respectively. Amino acid sequence analysis confirmed the highly purified protein as human MxA protein.

The protein concentration of the MxA protein was determined by the Bradford method (25) using the Bio-Rad DC Protein Assay Kit (Bio-Rad Laboratories, CA) with BSA as the standard, and was found to be 0.257 mg/ml.

The MxA protein solution was diluted to 24 ng/ml with the dilution buffer, divided into 1 ml each in a brown vial and lyophilized at –50°C for 48 h. After displacement of the atmospheric gases in the vial by N_2, the vial was sealed and the lyophilized MxA protein was stored at 4°C until use. When used in the ELISA, 1 ml of distilled water was added to the vial to resuspend the MxA protein, and the concentration of this MxA protein was determined to be 24 ng/ml.

To prepare the standards, 24 ng/mL of MxA protein was serially diluted with the dilution buffer and 0.38, 0.75, 1.50, 3.00, 6.00, 12.00, and 24.00 ng/ml of standards were prepared. The results of the ELISA were expressed in ng/ml of whole blood as determined by the standards.

Enzyme-linked immunosorbent assay

Twenty-five microliter of whole blood was diluted with 225 μl of the dilution buffer for cell lysis. One hundred microliter of the diluted sample or standard was added to each well of the antibody-coated plates and the plate was then incubated for 30 min at room temperature. After washing the plate five times with the washing buffer (PBS containing 0.05% [v/v] Tween-20), 100 μl of HRP-labeled KM1124 conjugate was added to each well, and the plate was incubated for 30 min at room temperature. After washing the plate five times with the washing buffer, 100 μl of TMBZ solution was added to each well, and the plate was then incubated for 10 min at room temperature. To stop the enzyme reaction, 50 μl of 0.5 mol/l H_2SO_4 was added, and the absorbance at 450 nm was measured with an MTP-120 plate reader (Corona Electric Co. Ltd., Tokyo, Japan).

Interference Study

Interference by lipids, direct bilirubin, indirect bilirubin, hemoglobin, and various anticoagulants was examined by the addition of the test metabolite to aliquots of whole blood. Metabolites and chemicals to be tested for interference were obtained from commercial sources at the highest purity available. Interference by lipids was tested using Intralipid® (Kabivitrum, Inc., California). Interference by heterophilic antibodies was tested using HAMA Sera® (Roche Diagnostics GmbH).

Statistical Analysis

Data are expressed as mean ± SD or median. Differences were examined by the Student's *t*-test or the Mann–Whitney *U* test. Receiver operating characteristic (ROC) analyses were done using the method of Hanley and McNeil (26). Computer analysis was performed with the Statcel package (OMS, Ltd., Saitama, Japan).

TABLE 1. Properties of Anti-MxA Monoclonal Antibodies

		Western blotting		Immunocytostaining		Immunoprecipitation				
KM No.	Type	76 kDa	30 kDa	IFNα	Inf	10–662	10–468	10–297	10–220	Kd
1122	IgG1	+	−	−	ND	ND	ND	ND	ND	
1123	IgG1	+	+	−	ND	ND	ND	ND	ND	ND
1124	IgG1	+	−	+	+	+	+	+	−	1.9×10^{-6}
1125	IgG1	+	−	−	ND	ND	ND	ND	ND	ND
1126	IgG1	+	−	+	−	+	+	+	+	1.8×10^{-6}
1127	IgG1	+	−	−	ND	ND	ND	ND	ND	ND
1128	IgG2a	+	+	−	ND	ND	ND	ND	ND	ND
1129	IgG1	+	−	ND	ND	ND	ND	ND	ND	
1130	IgG2a	+	+	−	ND	ND	ND	ND	ND	
1131	IgG1	+	+	−	ND	ND	ND	ND	ND	ND
1132	IgG2a	+	+	+	+	+	−	−	−	ND
1133	IgG1	+	+	−	ND	ND	ND	ND	ND	ND
1134	IgG2a	+	+	−	ND	ND	ND	ND	ND	ND
1135	IgG1	+	+	+	+	+	+	+	+	1.8×10^{-7}

ND, not done; IFNα, interferon α-stimulated cells; inf, influenza virus-infected cells.
+: positive result; −: negative result.

RESULTS

Mouse Hybridomas

Several hundred mouse hybridomas were screened by ELISA for the presence of antibodies against human recombinant MxA protein. Consequently, 14 mAb-producing lines, designated as KM1122~1135 were selected for expansion and used to produce ascites. mAb purified from ascites were used in all subsequent experiments to detect MxA protein employing the ELISA.

Characterization of mAb

As shown in Table 1, western blot analysis demonstrated all the mAb selected recognized the 76-kDa MxA protein. In addition, KM 1123, 1128, 1130–1135 also reacted with a 30-kDa band, a degradation product of the MxA protein. Immunocytostaining study said that KM1124, KM1126, KM 1132, and KM1135 could recognize the MxA protein from interferon α-stimulated cells but not unstimulated cells and additionally, KM1124, KM1132, and 1135 also reacted the MxA protein from the influenza virus-infected cells. The binding site of each mAb was determined based on the measured molecular weight. As a result, it was revealed that the anti-human MxA protein mAb KM1126 and KM1135 have a binding site at amino acids 10–220, KM1124 at amino acids 220–297, and KM1132 at amino acids 468–662, counting from the amino terminus of the MxA protein.

KM1124 and KM1135 were chosen for ELISA because of its binding site and reactivity against the cell induced by interferon α and viral infection. These antibodies had a suitable dissociation constant (Kd) to develop the ELISA system for measurement of MxA protein in whole blood.

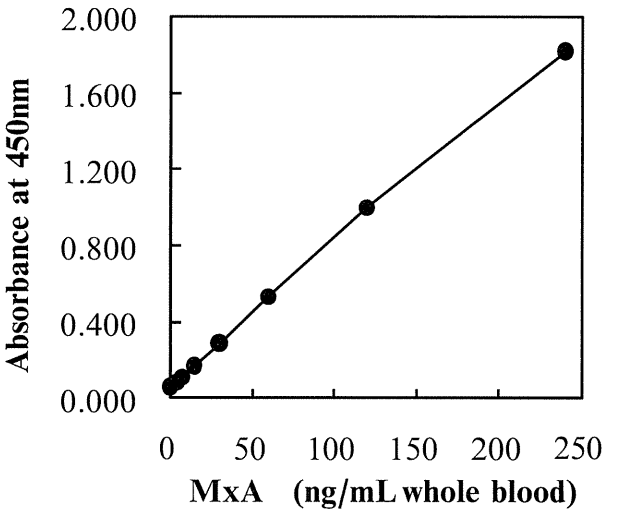

Fig. 1. Standard curve for the MxA protein-specific ELISA. Each point represents the mean of two measurements.

ELISA for Detection of MxA Protein

A sandwich ELISA for whole blood MxA protein was performed with a 96-well microtiter plate as the solid phase, KM1135 antibody as the capture antibody, KM1124-HRP conjugate as the second enzyme-labeled antibody, and TMBZ solution as the enzyme substrate. Figure 1 is a typical calibration curve generated by plotting the absorbance at 450 nm vs. the concentration of each standard.

Specificit

To confirm that the MxA protein-specific ELISA was clinically useful, T98G cells were stimulated with

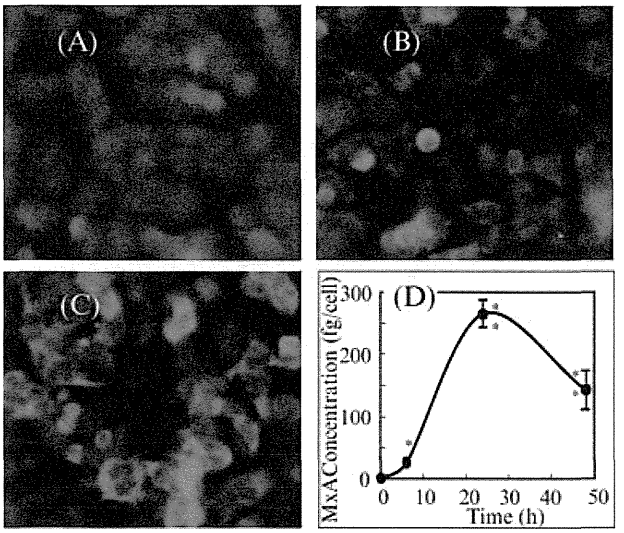

Fig. 2. Immunocytostaining and expression of MxA protein in interferon α-stimulated 98TG cells. (A) Immunocytostaining of MxA protein in 98TG cells before stimulation with interferon α, (B) after 2-h stimulation, (C) after 6-h stimulation, (D) concentration of MxA protein in 98TG cells stimulated with interferon α at 0 h. Each point represents the mean ± SD of three cultures. * and **: Significantly different from the value at 0 h, $P < 0.05$ and $P < 0.001$, respectively.

interferon α, and the MxA protein in the cell lysate was measured between 0 and 50 h. By immunocytostaining with fluorescent-labeled antibody, MxA protein was confirmed in the cytoplasm of interferon α-stimulated T98G cells (Fig. 2A, B, and C). This ELISA detected MxA protein in the cell lysate concomitant with the appearance of MxA protein in the cytoplasm of interferon α-stimulated cells (Fig. 2D).

Dilution Analysis

Whole blood samples serially diluted gave results close to linearity (Fig. 3), indicating that the assay was quantitative and confirming parallelism between the standard and whole blood.

Interference

Whole blood samples containing low (47 ng/ml), medium (105 ng/ml), and high (193 ng/ml) MxA protein concentrations were supplemented with potential interfering agents at various concentrations. There was no substantial interference from lipids up to 5 g/l (in terms of total glycerol), from hemoglobin up to 15 g/l, from direct and indirect bilirubin up to 200 mg/l, heparin up to 400 mg/l, NaF up to 4 g/l, EDTA up to 2 g/l, and sodium citrate up to 10 g/l. Human anti-mouse antibody positive serum was serially added to normal human whole blood and the whole blood was used for testing for interference

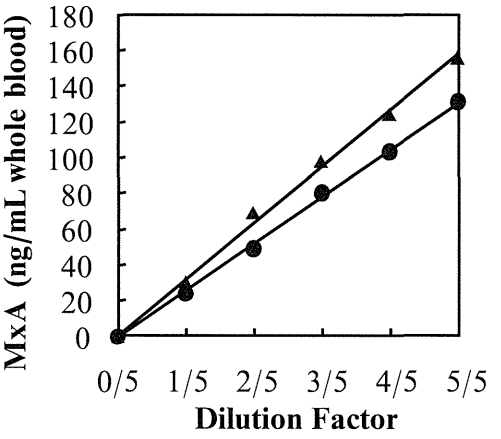

Fig. 3. Dilution curve for MxA protein in whole blood.

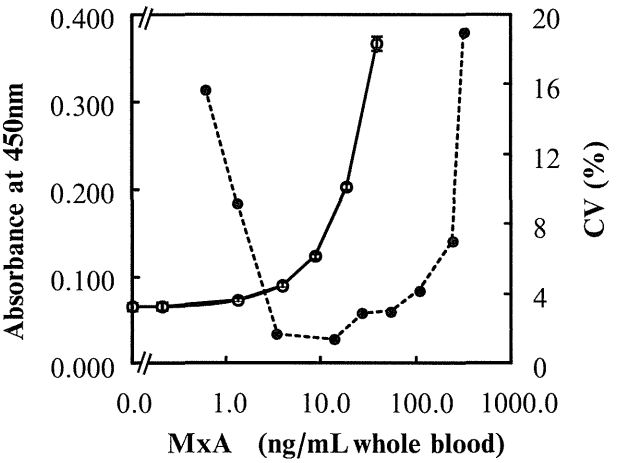

Fig. 4. Detection limit and practical assay range of MxA protein by ELISA. Each point of the detection limit represents the mean ± 2 SD of five measurements (○). Each point of the practical assay range represents the coefficients of variation (CV) value of six measurements (●).

of heterophilic antibodies. No false-positive signals were observed.

Detection Limit and Practical Assay Range of MxA Protein in Human Whole Blood

The detection limit of MxA protein in human whole blood by the ELISA was determined. Human whole blood containing MxA protein was serially diluted and used for testing. A significant difference of each serially diluted sample, compared to 0 ng/ml was confirmed by a Student's t-test ($n = 5$, $P < 0.001$). Figure 4 shows that 1.3 ng/ml of MxA protein in whole blood could be detected within 90 min by this assay. With the standard as the test sample, 0.13 ng/ml could be detected without pretreatment with the dilution buffer. The working range of the assay was established by calculating the coefficients of